

# Thermal Particle and Photon Production in $Pb + Pb$ Collisions with Transverse Flow.

J. Cleymans, K. Redlich\*, D.K. Srivastava\*\*

*Department of Physics, University of Cape Town, Rondebosch 7700, South Africa*

Particle and photon production is analyzed in the presence of transverse flow using two approximations to describe the properties of the hadronic medium, one containing only  $\pi, \rho, \omega$ , and  $\eta$  mesons (*simplified equation of state*) and the other containing hadrons and resonances from the particle data table. Both are considered with and without initial quark gluon plasma formation. In each case the initial temperature is fixed by requiring  $dN_{ch}/dy \sim 550$  in the final state.

It is shown that most observables are very sensitive to the equation of state. This is particularly evident when comparing the results of the simplified equation of state in the scenarios with and without phase transition. The hadronic gas scenario leads to a substantially higher rate for the  $p_T$ -distribution of all particles.

In the complete equation of state with several hundreds of hadronic resonances, the difference between the scenarios with and without phase transition is rather modest. Both photon and particle spectra, in a wide  $p_T$  range, show very similar behavior. It is therefore concluded that from the  $p_T$  spectra it will be hard to disentangle quark gluon plasma formation in the initial state. It is to be stressed however, that there are conceptual difficulties in applying a pure hadronic gas equation of state at SPS-energies. The phase transition scenario with a quark gluon plasma present in the initial state seems to be the more natural one.

## I. INTRODUCTION

The direct experimental evidence for transverse flow in relativistic heavy ion collisions is weak and in many models it is even ignored completely. The evidence is mainly “circumstantial” [1], however, in all recent analyses of particle ratios it is impossible to ignore transverse flow without running into contradictions [2–6]. There has therefore been a lot of interest recently in analyzing the effects of flow more thoroughly [7–10].

A clear illustration of the effects of transverse flow is shown in figures 1 and 2. Figure 1 shows the average transverse momentum as a function of the freeze-out temperature in the absence of flow. Clearly if the freeze-out temperature is very high the outgoing particle will be very energetic and the average transverse momentum will be large accordingly. However, in the presence of transverse flow this is changed completely as shown in figure 2 where we plot again the transverse momentum as a function of freeze-out temperature but this time taking into account transverse flow. Compared to figure 1 the behaviour is changed totally : the higher the freeze-out temperature, the lower the transverse momentum, just the opposite from figure 1. The explanation for this is very simple. If the freeze-out temperature is very low, the hadronic system will be long-lived because it takes a longer time to cool down. Since the lifetime is long, the transverse expansion will act for a long time, one ends up with a large transverse momentum. The freeze-out temperature is no longer the deciding factor as it is in figure 1 but the lifetime of the hadronic system becomes more important. Similarly the presence of a phase transition will also change the transverse expansion substantially because during the phase transition the speed of sound becomes zero and this will slow considerably the transverse expansion. We thus expect the distribution in transverse momentum to be strongly affected by the lifetime of the hadronic system and by the presence (or absence) of a phase transition.

It is well known that the equation of state has an important effect on the transverse expansion of hot hadronic matter [8,10,11]. In particular, the occurrence of a phase transition considerably changes the development and the speed with which the transverse expansion occurs [7].

In models of hydrodynamic flow it is unnatural to have an instantaneous freeze-out of all particles. This was recently emphasized in reference [9] and follows simply from the fact that the freeze-out temperature will affect particles in the center of the collision at a later stage than particles which are at the edges of the hadronic system. It takes some time for the cooling to propagate through the system and thus the different freeze-out times. In kinetic models it is even unnatural for particles of different types to freeze out at the same time because of their different mean free paths. This is illustrated in figure 3 (based upon reference [12]) showing the mean free paths of pions and kaons as a function of temperature. In the remainder of this paper we will not take this into account and concentrate on the

effects of the transverse expansion on particle production. We consider particles to freeze-out when their environment reaches a certain temperature and we thus ignore differences between the types of particles. In this paper we would like to investigate in detail the influence of transverse expansion on as many quantities as possible. This in turn affects the transverse momentum distribution. It is the purpose of this paper to investigate systematically the effect of four different choices on the transverse expansion of hot hadronic matter.

For the hadronic matter we will use two approximations to describe the medium. In the first one only a small number of mesons ( $\pi, \rho, \omega$ , and  $\eta$ ) is used (*simplified equation of state*) while in the second one all hadrons listed in the particle data table [14] are used. Both equations of state will be considered with, and without, a quark gluon plasma in the initial state. In all four cases considered the initial temperature is fixed by requiring  $dN_{ch}/dy \sim 550$  in the final state, assuming  $dN/dy = 1.5 \times dN_{ch}/dy$  and imposing entropy conservation during the expansion. The initial thermalization time is assumed to be  $\tau_0 \sim 1\text{fm}$ .

Most physical observables (but not all) are very sensitive to the equation of state, and the assumptions made about the nature of the initially created system. This is particularly evident when comparing the simplified equation of state in the scenarios with and without phase transition. Here the purely hadronic gas scenario leads to substantially larger  $p_T$  distributions for all particles (including photons). This is mainly due to the very different initial temperatures arising from the fact that the freeze-out temperature is the same in all scenarios.

For the equation of state with several hundreds of hadrons the difference between the scenario with, and without, phase transition is almost non-existent. Thus one concludes that it will be hard to prove the presence of a quark gluon plasma in the initial state. One has to stress, however, that the assumption of an equation of state with the phase transition scenario and quark gluon plasma formation in the initial state is the more natural one. This is because there are conceptual difficulties in applying a purely hadronic gas equation since a temperature  $T \sim 200\text{ MeV}$  leads to a particle density of the order of  $2\text{--}3/\text{fm}^3$ . When considering hadrons as extended objects with a radius  $R \sim 1\text{ fm}$ , this is clearly not acceptable.

In section 2 we briefly review the hydrodynamic equations. In section 3 we discuss the equation of state in detail. Results on the hadronic spectra (pions and kaons) are presented in section 4. Photons are discussed separately in section 5. The  $\eta/\pi^0$  ratio is discussed in section 6. In section 7 we discuss and summarize our results.

## II. FORMULATION OF HYDRODYNAMICS

The standard starting point for hydrodynamics is the conservation law for the energy momentum tensor [13]

$$\partial^\mu T_{\mu\nu} = 0 \quad (2.1)$$

with

$$T_{\mu\nu} = (\epsilon + P)u_\mu u_\nu - g_{\mu\nu}P \quad (2.2)$$

with the 4-velocity  $u_\mu$  given by :

$$u_\mu = \frac{1}{\sqrt{1-v_r^2}} (\cosh \eta, v_r \cos \phi, v_r \sin \phi, \sinh \eta). \quad (2.3)$$

Here  $v_r$  is the transverse (radial) velocity,  $\eta$  is the space-time rapidity defined as

$$\eta = \frac{1}{2} \ln \frac{t+z}{t-z}. \quad (2.4)$$

The conservation law  $\partial_\mu T^{\mu 0} = 0$  leads to the following equation at zero rapidity :

$$\begin{aligned} \frac{\partial}{\partial \tau} \left[ \frac{\epsilon + P}{1 - v_r^2} - P \right] &= - \frac{\partial}{\partial r} \left[ \frac{\epsilon + P}{1 - v_r^2} \right] \\ &\quad - \frac{\epsilon + P}{1 - v_r^2} \left[ \frac{v_r}{r} + \frac{1}{\tau} \right]. \end{aligned} \quad (2.5)$$

For numerical purposes is best to rewrite this equation in the form

$$\frac{\partial}{\partial \tau} T_{00} + \frac{\partial}{\partial r} [v_s T_{00}] = - [T_{00} + P] \left[ \frac{v_r}{r} + \frac{1}{\tau} \right] \quad (2.6)$$

where

$$v_s = \frac{\epsilon + P}{1 - v_r^2} v_r \Big/ \left[ \frac{\epsilon + P}{1 - v_r^2} - P \right] \quad (2.7)$$

This can be readily used in one of the numerical algorithms which have been developed for solving hydrodynamical equations.

Similarly the equation  $\partial_\mu T^{\mu z} = 0$  leads to

$$\begin{aligned} \frac{\partial}{\partial \tau} \left[ \frac{\epsilon + P}{1 - v_r^2} v_r \right] &= - \frac{\partial}{\partial r} \left[ \frac{\epsilon + P}{1 - v_r^2} v_r^2 \right] \\ &\quad - \frac{\partial P}{\partial r} \\ &\quad - \frac{\epsilon + P}{1 - v_r^2} v_r \left[ \frac{v_r}{r} + \frac{1}{\tau} \right] \end{aligned} \quad (2.8)$$

which can be rewritten as

$$\frac{\partial}{\partial \tau} T_{0r} + \frac{\partial}{\partial r} [v_r T_{0r}] = - \frac{\partial P}{\partial r} - T_{0r} \left[ \frac{v_r}{r} + \frac{1}{\tau} \right]. \quad (2.9)$$

Equations (6) and (10) determine the time evolution of  $T_{00}$  and  $T_{0r}$ . From these two we can then determine the energy density using the following implicit equation

$$\frac{T_{0r}^2}{T_{00} + P(\epsilon)} = T_{00} - \epsilon. \quad (2.10)$$

The pressure is then determined from the equation of state. The velocity is determined from  $T_{00}$  and  $T_{0r}$ . The time evolution of all the thermodynamic quantities can thus be determined.

### III. EQUATION OF STATE

We discuss in detail four different scenarios. In the first one we consider a gas composed of a limited set of mesonic resonances, namely,  $\pi, \rho, \omega$  and  $\eta$  (simplified equation of state) while in the second case we use a gas containing all resonances listed in the particle data table [14]. Each one of these two cases is then considered with or without a phase transition to a quark-gluon plasma. As has been noted previously the presence of a phase transition substantially alters the transverse expansion and the distribution in transverse momentum is affected accordingly. The phase transition slows down the transverse expansion and the average transverse momentum is thus lowered. The energy density as a function of temperature is shown in figure 4. The speed of sound is given in figure 5 as a function of the temperature while the particle density is shown in figure 6. The pressure is given in figure 7. Note that all these quantities are “raw” in the sense that no corrections have been made for interactions not even in their crudest forms like e.g. excluded volume effects.

The results in figures 4-7 already show the main differences in the thermodynamics of all four equations of state. At the critical temperature, which we assume to be  $T_c = 160$  MeV, the effective number of degrees of freedom increases by more than a factor of two when going from the simplified to the complete particle input in hadronic matter. This naturally reduces the lifetime of the system in the mixed phase. A steeper increase of pressure versus energy density seen in figure 7 for the simplified equation of state implies a higher value for the speed of sound in figure 5.

The functional dependence of the temperature on proper time, for a purely longitudinal expansion according to Bjorken hydrodynamics [15] seen in figure 8 shows that with the simplified equation of state with no phase transition one needs a temperature  $T \approx 320$  MeV to reproduce the final state entropy. For the complete equation of state and in the scenario with phase transition the temperature is reduced to the value of  $\approx 210$  MeV. Thermal particle and photon production is very sensitive to the temperature value, thus one should see a very different behavior of particle and photon spectra depending on the particle input in the equation of state. In figure 8 one can also see that the lifetime of the mixed phase is much longer for the simplified than for the complete equation of state. These results reflecting the effective number of degrees of freedom at  $T_c$ , imply that for the simplified version of the equation of state the thermal photon production is mostly due to the contribution of the mixed phase. Including resonances changes this result, reducing the lifetime of the mixed phase and increasing production from the pure hadronic phase. For

small and intermediate photon momenta the quark- gluon plasma contribution to the overall rate is negligible due to its short lifetime and not to the high initial temperature.

The freeze-out surface calculated in figures 9-10 shows a very strong dependence on the value of the freeze-out temperature, which in the context of hydrodynamical models is considered a free parameter. There are some dynamical restrictions on the values of  $T_f$  due to particle scattering in the medium. One can see in figure 3 that for pions a freeze-out temperature in the range of 100-160 MeV is still allowed as it leads to a mean free path which is of the order of the radius of the  $Pb$  nucleus. Clearly the freeze-out time is small for particles close to the surface and largest for the ones close to the center. The higher initial temperature leads naturally to a longer lifetime. For the scenario with phase transition and simplified equation of state the freeze-out time is the longest one. This is mostly a reflection of the long-lived mixed phase. All the above features are contained in figures 9-10.

#### IV. RESULTS

The transverse momentum distribution of  $\pi^+$  is shown in figure 11a for the case where a phase transition occurs at a temperature of  $T_c = 160$  MeV. In figure 11b we show the same in the absence of phase transition. By comparing the two figures it is clear that the absence of a phase transition leads to much higher transverse momenta. In figures 12 we show the distribution of  $\pi^+$  for the case where the hadronic gas contains all known resonances. The main difference between the scenarios is that the gas containing the full set of resonances is much more sensitive to the freeze-out temperature.

Figures 13 and 14 show the distributions in transverse mass for the  $K^+$ . The highest transverse momenta are seen in figure 13b where we have no slowing down of the transverse expansion due to the phase transition. Figures 14a and 14b both show lower transverse momenta than figures 13a and 13b but they also show a greater sensitivity to the freeze-out temperature. This is again due to the presence of large numbers of kaons resulting from decays of heavy resonances.

Figure 15 summarizes the average transverse momenta for the full resonance gas. In figure 15a we show this for the scenario where no phase transition occurs, figure 15b shows the case where we do have a transition. The phase transition results in much lower transverse momenta for the outgoing particles.

#### V. THERMAL PHOTON YIELD

In the previous section we have analyzed the influence and the role of the equation of state on the properties and behavior of particle spectra. Particle production, however, is not the only observable which could give some insight into the nature and the structure of the hot hadronic matter which is produced in ultra-relativistic heavy ion collisions. In particular photons are a very promising probe in the experimental search for the QGP formation in A-A collisions [13,16–22]. This is mainly because the mean free path of a photon in a thermal medium is expected to be larger than the size of the medium, at least when the energy of the  $\gamma$  is not too small. Thus, photons, once produced inside the medium will carry direct information about its nature and its properties. Photons are radiated both from the plasma and from the hadronic phase. Thus, to find the possible kinematical window where photon production from QGP overwhelms the hadronic contribution, one needs to study different contributing reactions to the overall thermal rate. Clearly, the thermal photon spectra are influenced by the equation of state of hot hadronic matter as well. In this section we will discuss the extent to which the equation of state could modify the thermal photon yield. We will restrict our discussion to hard photons with energies larger than the temperature of the medium

The Born calculation of the hard photon rate with a bare internal quark propagator for the  $\bar{q}q \rightarrow g\gamma$  and  $qg \rightarrow q\gamma$  processes leads to divergent production rate in the limit of vanishing quark mass [23]. It has been shown, however, [24,25] that in the framework of the re-summed perturbative expansion of Braaten and Pisarski [26] the mass singularities due to the exchange of massless quarks are shielded by Landau damping effects. In a QGP of temperature  $T$ , the thermal photon rate has been found to be [24,25]:

$$E \frac{dN^\gamma}{d^4x d^3q} \simeq \frac{e_q^2 \alpha \alpha_s}{2\pi^2} T^2 \exp(-E/T) \ln\left(\frac{0.23E}{\alpha_s T}\right), \quad (5.1)$$

with  $\alpha_s(T)$  being the strong coupling constant which following ref. [27] we have parameterized as:

$$\alpha_s(T) = \frac{6\pi}{(33 - 2n_f) \ln(8T/T_c)} \quad (5.2)$$

where the critical temperature is taken to be  $T_c = 160$  MeV. We used  $n_f = 2$  for the simplified equation of state and  $n_f = 3$  in the case of all hadrons.

The above result for the thermal photon rate in a plasma is only valid for hard  $E > T$  photons, and cannot be applied to the soft part of the spectrum. For soft photons ( $E \sim gT$ , where  $g$  is the QCD coupling constant), one needs to re-sum not only the propagators but also the dressed vertices. The detailed calculation of the soft photon rate, performed in [28], show that the Braaten-Pisarski re-summation does not lead to a finite result, free from mass singularities. Moreover, in [29] it was indicated that, the Braaten-Pisarski re-summed contribution is subleading, as there is a set of singular bremsstrahlung type diagrams which dominate the soft photon rate.

Having in mind the above problems we will analyze only the production of hard photons. The contribution from quark bremsstrahlung [30] is also neglected in our discussion.

In the hadronic gas at temperature  $T$  the thermal photon rates were analyzed in [30] where all contributions originating from the two loop approximation of the real photon self energy using model with  $\pi - \rho$  interactions were calculated. The dominant contribution to the photon rate was found to be Compton  $\pi\rho \rightarrow \pi\gamma$ , decay  $\rho \rightarrow \pi\pi\gamma$  and the annihilation  $\pi\pi \rightarrow \rho\gamma$ , processes. Moreover, for high enough temperature, the scattering and the decay of the  $A_1$  axial vector meson has been shown to play an essential role when discussing the thermal photon rate in a hadronic medium. All these contributing effects are included in our analysis of thermal photons originating from hadronic matter.

Having established the production cross sections, the photon  $p_T$ -spectrum is then obtained by convoluting the photon rates with the space-time history of the system as

$$\frac{dN}{d^2p_T dy} = \int \tau d\tau r dr d\phi d\eta \left[ f_Q q_0 \frac{dN^q}{d^4x d^3q} + (1 - f_Q) q_0 \frac{dN^\pi}{d^4x d^3q} \right] \quad (5.3)$$

where the function  $f_Q(r, \tau, \eta, \phi)$  describes the fraction of the quark gluon plasma in the system [23]. In the scenario without phase transition  $f_Q \equiv 0$ .

The numerical integration in the above equation is based on the hydrodynamical scheme summarized in our previous sections and described in more detail in ref. [13,32].

The results on photon yields in thermal expanding medium are shown in figures 16-17. In figure 16 the photon  $p_T$  spectra were calculated assuming the hadronic gas as composed of only few hadrons and resonances  $\pi, \rho, \omega, \eta$ . As it can be seen in fig.16 the photon yield in the scenario without phase transition exceeds substantially the result obtained under the assumption of a QGP formation in the initial state. This dramatic difference arises mostly from the very different initial temperature required in both scenarios to reproduce the same final state particle multiplicity. As it can be deduced from figure 8 one needs the initial temperature  $T_0 \sim 318$  MeV in hadronic medium and  $T_0 \sim 210$  MeV in a QGP to get  $dN_{ch}/dy \sim 550$ . As the thermal production is a strongly increasing function of  $T$ , larger temperatures naturally lead to a higher photon yield. We have to note, however, that at high enough  $T$  the approximation of the hadronic equation of state as being composed only from very few hadrons is not realistic. When increasing the temperature beyond 100 MeV the contribution of heavier particles and resonances has to be included. This can already be seen in figure 4 where at  $T \sim 150$  MeV the contribution of resonances increases the energy density of a thermal medium by a factor two. Thus it is clear that in modeling the equation of state of hadronic matter we should not neglect heavier resonances.

In figure 17 we have made a similar calculation to the one presented in figure 16 but this time including all resonances in the hadronic equation of state. One can see in figure 17 that this time, contrary to figure 16, there is no difference between the scenario with and without phase transition. In both cases the hydrodynamical model leads to almost the same result for the photon  $p_T$  distribution in a wide  $p_T$  range. This is because, contrary to figure 16, the initial temperature and the lifetime of the systems are quite similar. The only difference between both scenarios is thus the photon production cross section. It was shown, however, [25] that at fixed temperature the photon emissivity of the QGP plasma and hadronic matter is quantitatively very similar. That is why also in the expanding medium the differences between both scenarios are rather modest as seen in figure 17. A similar conclusion was reached recently in reference [10].

Discussing photon production in the resonance gas we have only included photons originating from the processes involving pions, rho and  $A_1$  vector mesons. Thus, the results in fig.17 should be considered as the lower limit for thermal photon production. The contribution of other hadrons, present in the hadronic phase, will certainly increase the photon rate both in the scenario with and without phase transition. We do expect, however, that the relative difference between these scenarios will not be much affected by the additional hadronic processes for direct photon production.

We should point out that the scenario which does not involve a phase transition has very high particle density in the initial stages. One could attempt to correct for this by including the finite size corrections using one of the many

Ansätze in the literature for this purpose. We have verified that none of the Ansätze remain valid at  $\tau_i = 1 \text{ fm}/c$ , when the volume is only about  $160 \times \Delta y \text{ fm}^3$ . Neglecting the finite volume, this means more than 10 hadrons/ $\text{fm}^3$  in the case of the hadronic gas with only  $\pi$ ,  $\rho$ ,  $\omega$ , and  $\eta$  mesons, and more than 3 hadrons/ $\text{fm}^3$  in the case of exhaustive list of resonances (see figure 6). This criticism also applies to the case of particle spectra as well.

As a closing remark we have to point out however that there is a huge non-thermal background due to hadron decays, mainly  $\pi^0$  and  $\eta$ , which give substantial contributions to the overall measured photon distributions. In order to disentangle the quark-gluon plasma presence, one needs of course first to see thermal production to exceed the non-thermal background. Recent comparisons of thermal hydrodynamical models [22,31] with experimentally measured photon yield by WA80 collaboration in S-Au collisions at SPS energy has shown a large contribution of thermal photons. Thus, there are very good perspectives to disentangle the QGP in A-A collisions measuring photon spectra.

## VI. $\eta/\pi$ RATIO

All measurements of single photons in a given  $p_T$  window necessarily entail a precise determination of the decay photons from  $\pi^0 \rightarrow \gamma\gamma$  and  $\eta \rightarrow \gamma\gamma$  in the same window. This in turn provides the spectra of  $\pi^0$  and  $\eta$  particles, which are often used to provide a confirmation of the so-called “ $m_T$ -scaling”. The  $m_T$ -scaling plays an important role in these studies by providing a basis for extrapolation of the  $p_T$  spectra of the  $\eta$  into unmeasured regions and also to estimate the  $p_T$  spectra for other unmeasured hadrons which give small photon decay contributions.

In figures 18 and 19 we show the  $\eta/\pi^0$  ratio as a function of transverse momentum for different values of the freeze-out temperature. Again we compare the cases with and without phase transition and also the resonance-rich versus the resonance poor hadronic gas. We note that in the case where the gas contains only a few resonances, this ratio rises more rapidly when there is a phase transition. The results are essentially identical for the phase transition and the no phase transition case when we have the full list of hadrons describing the hadronic matter.

## VII. CONCLUSIONS

We have analyzed particle and photon production in strongly interacting matter as produced in ultra-relativistic heavy ion collisions. Using models with transverse flow and a longitudinally boost invariant expansion in the  $z$ -direction we have studied the dependence of the results on the equation of state. For the hadronic matter we used two different approximations to describe the thermodynamical properties of the medium. The model with  $\pi, \rho, \omega$ , and  $\eta$  mesons (*simplified equation of state*) and the model with all hadrons and resonances from the particle data table. Both these equations of state have been considered with, and without, quark gluon plasma formation in the initial state. In all cases the initial temperature was fixed by requiring  $dN_{ch}/dy \sim 550$  in the final state and assuming entropy conservation during the expansion. The initial thermalization time  $\tau_0 \sim 1 \text{ fm}$  was also assumed.

It was shown that most physical observables derived within the above hydrodynamical model for the expansion dynamics are very sensitive to the equation of state, and assumptions were made about the nature of the initially created fire cylinder. This is particularly evident when comparing the results of the simplified equation of state in the scenario with, and without, phase transition. Here the hadronic gas scenario leads to a substantially higher rate for the  $p_T$  distribution of both particles and photons. This is entirely due to a very different initial temperature required in both of these cases. In any case the simplified hadronic equation of state with only a few particles becomes unrealistic at higher temperatures and can lead to misleading conclusions if applied at the high temperatures, implicit in the no phase transition scenario.

When assuming more complete equation of state with a few hundred hadrons and resonances the difference between the scenario with, and without, phase transition is rather modest. Both photon and the particle spectra in the wide  $p_T$  range, show quantitatively very similar behaviour. Some small excess of the yield in the scenario without phase transition reflects slightly higher initial temperature than required for the quark gluon plasma formation in the initial state. Thus, from the above, one could conclude that from the measured  $p_T$  spectra it would be rather hard to disentangle the quark gluon plasma formation in the initial state. We have to repeat, however, that there are conceptual difficulties in applying only hadron gas equation of state for the conditions of the SPS-energy. At the temperature  $T \sim 200 \text{ MeV}$ , required to satisfy measured final state pion multiplicity in Pb-Pb collisions, we are ending up with a particle density of the order of  $2\text{--}3/\text{fm}^3$ . When considering hadrons as extended objects of the radius  $R \sim 1 \text{ fm}$ , these initial conditions are not acceptable. This is in the spirit of the Hagedorn model which leads to the appearance of the limiting temperature above of which the hadron concept does not make any sense. Thus, from the point of view of principle, for the SPS energy the assumption of the equation of state with the phase transition scenario and the quark gluon plasma formation in the initial state seems to be more natural.

Discussing particle spectra for the conditions of Pb-Pb collisions at the SPS energy we have not made any comparisons with the existing experimental data of NA49 collaboration. The main reason for this was due to the simplification of our calculations which restrict us only to direct thermal particle production without taking into account the decay of resonances. This approximation is sufficient to study the role of the equation of state but is not adequate to make any comparisons with the experimental data. It is quite clear that as long as the temperatures remain small compared to the pion mass, one may use either of the hadronic equations of state as the contributions of the heavier mesons will be negligible. As the temperature rises, the contribution of the heavier resonances will increase. If we limit the number of allowed particles to a small number, as in the simplified equation of state, the temperature becomes very high for a given entropy density. On the other hand, the equation of state having the full hadronic spectrum implies a complete chemical equilibrium amongst all hadrons, which may or may not be achieved. We have already stated repeatedly that both equations of state imply too high a density in the initial stage for the case without phase transition. It is of considerable interest to note that if we assume the initially produced matter to be in the QGP phase, then the results for the thermal photons and also for the other quantities that we have studied differ only marginally for the different equations of state considered.

In summary, we have shown that most observables are very sensitive to the equation of state. For the simplified equation of state the hadronic gas scenario (without phase transition) leads to the highest rate for the  $p_T$ -distribution of all particles. Using the equation of state with all particles listed in the particle data booklet, the difference found between the scenarios with and without phase transition is very modest. Both photon and particle spectra, in a wide  $p_T$  range, show very similar behavior. We therefore conclude that if we can reconcile with very large particle densities in the hadronic gas description, then from the  $p_T$  spectra alone, it will be hard to prove the presence of a quark gluon plasma.

#### ACKNOWLEDGMENTS

We would like to thank Kevin Haglin for supplying us with the code used for figure 3. We also thank Vesa Ruuskanen for his help with solving the hydrodynamic equations numerically. One of us acknowledges financial support from the University of Cape Town (URC) and the Foundation for Research Development (FRD, Pretoria). Two of the authors (K.R. and D.K.S.) would like to thank the warm and generous hospitality of the University of Cape Town where this project was conceived and largely executed. K.R. also acknowledges partial support of the Gesellschaft für Schwerionenforschung (GSI) and the Committee of Research Development (KBN 2-P03B-0998).

- 
- \* Gesellschaft für Schwerionenforschung (GSI), D-64220 Darmstadt, Germany.
  - \*\* Variable Energy Cyclotron Centre, 1/AF Bidhan Nagar, Calcutta 700 064, India.
  - [1] E. Schnedermann and U. Heinz, Phys. Rev., C50 (1994) 1675.
  - [2] J.M. Nelson et al., Nucl. Phys. A566 (1994) 217c; E. Andersen et al., Phys. Lett. B327 (1994) 433.
  - [3] J. Sollfrank, M. Gaździcki, U. Heinz and J. Rafelski, Z. Phys. C61 (1994) 394.
  - [4] J. Letessier, A. Tounsi, U. Heinz, J. Sollfrank and J. Rafelski, Phys. Rev. D51 (1995) 3408.
  - [5] J. Cleymans and H. Satz, Z. Phys. C57 (1993) 135.
  - [6] P. Braun-Munzinger, J. Stachel, J.P. Wessels and N. Xu, Phys. Lett. B344 (1995) 43.
  - [7] D.H. Rischke, S. Bernard and J.A. Mahrun, Nucl. Phys. A595 (1995) 346.
  - [8] D. K. Srivastava, S. Sarkar, P. K. Roy, D. Pal, and B. Sinha, Phys. Lett. B379 (1996) 54.
  - [9] S. Bernard, J.A. Mahrun, W. Greiner and D.H. Rischke, Frankfurt preprint UFTP-406, February 1996.
  - [10] J. Sollfrank, P. Huovinen, M. Kataja, P.V. Ruuskanen, M. Prakash and R. Venugopalan, Helsinki preprint HU-TFT-96-08, July 1996.
  - [11] D. K. Srivastava, B. Sinha, and C. Gale, Phys. Rev. C53 (1996) R567.
  - [12] K. Haglin and S. Pratt, Phys. Lett. B328 (1994) 255.
  - [13] See e.g. P.V. Ruuskanen, Acta Phys. Pol. B18 (1986) 551; “*Quark-Gluon Plasma*”, Ed. R. Hwa, World Scientific, Singapore, 1990, p.51 and also J.-P. Blaizot, J.-Y. Ollitrault, “*Quark-Gluon Plasma*”, Ed. R. Hwa, World Scientific, Singapore, 1990, p.393.
  - [14] *Review of Particle Properties*, Phys. Rev. D51 (1994) 1177.

- [15] J.D. Bjorken, Phys. Rev. D27 91982) 140.
- [16] A. Peshier, B. Kämpfer, O. P. Pavlenko, and G. Soff, Phys. Lett. B337 (1994) 235.
- [17] H. von Gersdorff, M. Kataja, L. McLerran, and P. V. Ruuskanen, Phys. Rev. D34 (1986) 794.
- [18] D. K. Srivastava, B. Sinha, M. Gyulassy, and X.-N. Wang, Phys. Lett. B276 (1992) 285.
- [19] S. Chakrabarty, J. Alam, D. K. Srivastava, B. Sinha, and S. Raha, Phys. Rev. D46 (1992) 3802.
- [20] D. K. Srivastava and B. Sinha, J. Phys. G18 (1992) 1467.
- [21] J. Alam, D. K. Srivastava, B. Sinha, and D. N. Basu, Phys. Rev. D48 (1993) 1117.
- [22] D. K. Srivastava and B. Sinha, Phys. Rev. Lett. 73 (1994) 2421; D. K. Srivastava and B. Sinha, Nucl. Phys. A590 (1995) 507c.
- [23] K. Kajantie and H.I. Miettinen, Z.Phys. C9 (1981) 341.; K. Kajantie and P.V. Ruuskanen, Phys. Lett. B121 (1983) 352;
- [24] R. Baier, H. Nakkagawa, A. Niegawa, and K. Redlich, Phys. Rev. D45 (1992) 4323.
- [25] J. Kapusta, P. Lichard and D. Seibert, Phys. Rev. D44 (1991) 2774.
- [26] E. Braaten and R. D. Pisarski, Phys. Rev. Lett. 64 (1989) 1338.
- [27] F. Karsch, Z. Phys. C38 (1988) 147
- [28] R. Baier, Y.L. Dokshitzer, A.H. Mueller, S. Peigne and D. Schiff, University of Bielefeld preprint BI-TP-96-21.
- [29] P. Aurenche, M. Fontannaz, J.P. Guillet, A. Kotikov and E. Pilon, Annecy, LAPP preprint ENSLAPP-A-595-96.
- [30] J. Cleymans, V.V. Goloviznin and K. Redlich, Phys. Rev. D47 (1993) 989; V.V. Goloviznin and K. Redlich, Phys. Lett. B319 (1993) 520; P. K. Roy, D. Pal, S. Sarkar, D. K. Srivastava, and B. Sinha, Phys. Rev. C **53**, 2364 (1995); D. Pal, P. K. Roy, S. Sarkar, D. K. Srivastava, and B. Sinha, “Soft electromagnetic radiations from relativistic heavy ion collisions”, submitted to Phys. Rev. C.; K. Haglin, C. Gale and V. Emelyanov, Phys. Rev. D47 (1993) 973.
- [31] J.J. Neumann, D. Seibert and G. Fai, Phys. Rev. C51 (1995) 1460; A. Dumitru, U. Katscher, J.A. Maruhn, H. Stöcker, W. Greiner and D.H. Rischke, Phys. Rev. C51 (1995) 2166; N. Arbex, U. Ornik, M. Plümer, A. Timmermann and R.M. Weiner. Phys. Lett. B354 (1995) 307; Yu. A. Tarsov, Phys. Lett. B379 (1996) R567.
- [32] K. Kajantie, M. Kataja, L. McLerran, and P. V. Ruuskanen, Phys. Rev. D34 (1986) 811.

FIG. 1. The average transverse momentum as a function of the freeze-out temperature in the absence of transverse flow.

FIG. 2a. The average transverse momentum as a function of the freeze-out temperature in the presence of thermal flow. The hadronic gas is made up of  $\pi, \rho, \omega$  and  $\eta$  mesons and no phase transition takes place.

FIG. 2b. The average transverse momentum as a function of the freeze-out temperature in the presence of thermal flow. The hadronic gas is made up of  $\pi, \rho, \omega$  and  $\eta$  mesons and a phase transition takes place at  $T_c = 160$  MeV.

FIG. 3. The mean free path of pions and kaons as a function of temperature (from reference [Kevin Haglin]).

FIG. 4. The energy density as a function of the temperature. The dashed line corresponds to a gas containing only  $\pi, \rho, \omega$  and  $\eta$  mesons (with and without phase transition to a quark gluon plasma). The full line takes into account all hadronic resonances with masses below 2.5 GeV (again with and without phase transition).

FIG. 5. The speed of sound (squared) as a function of temperature in a hadronic gas (without phase transition).

FIG. 6. The particle density as a function of temperature for two different scenarios explained in the text. No repulsive effects or excluded volume corrections have been taken into account.

FIG. 7. Pressure as a function of temperature for two different hadronic scenarios. No repulsive effects or excluded volume corrections have been taken into account.

FIG. 8. The temperature as a function of the proper time for the four different scenarios considered in the text.

FIG. 9a. The freeze-out time as a function of the radial distance  $r$  for different values of the freeze-out temperature  $T_f$ . The hadronic gas contains only  $\pi, \rho, \omega$  and  $\eta$  mesons and no phase transition takes place.

FIG. 9b. The freeze-out time as a function of the radial distance  $r$  for different values of the freeze-out temperature  $T_f$ . The phase transition occurs to a quark-gluon plasma occurs at  $T_c = 160$  MeV.

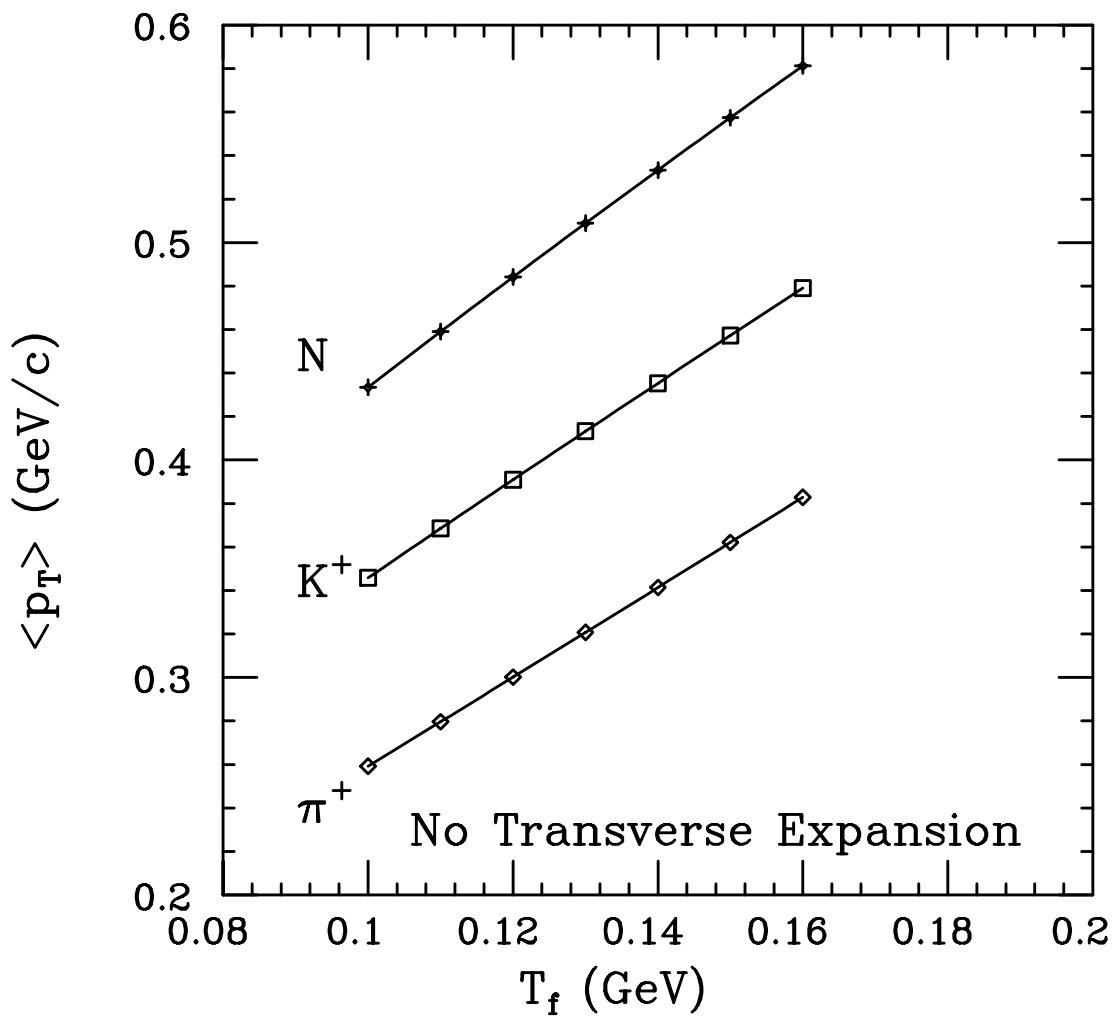
FIG. 10a. Freeze-out time as a function of the radial distance for a resonance gas without phase transition to a quark-gluon plasma. Different values of the freeze-out temperature are indicated.

FIG. 10b. Freeze-out time as a function of the radial distance  $r$  for a resonance gas with a phase transition occurring at  $T_c = 160$  MeV. Different values of the freeze-out temperature are indicated.

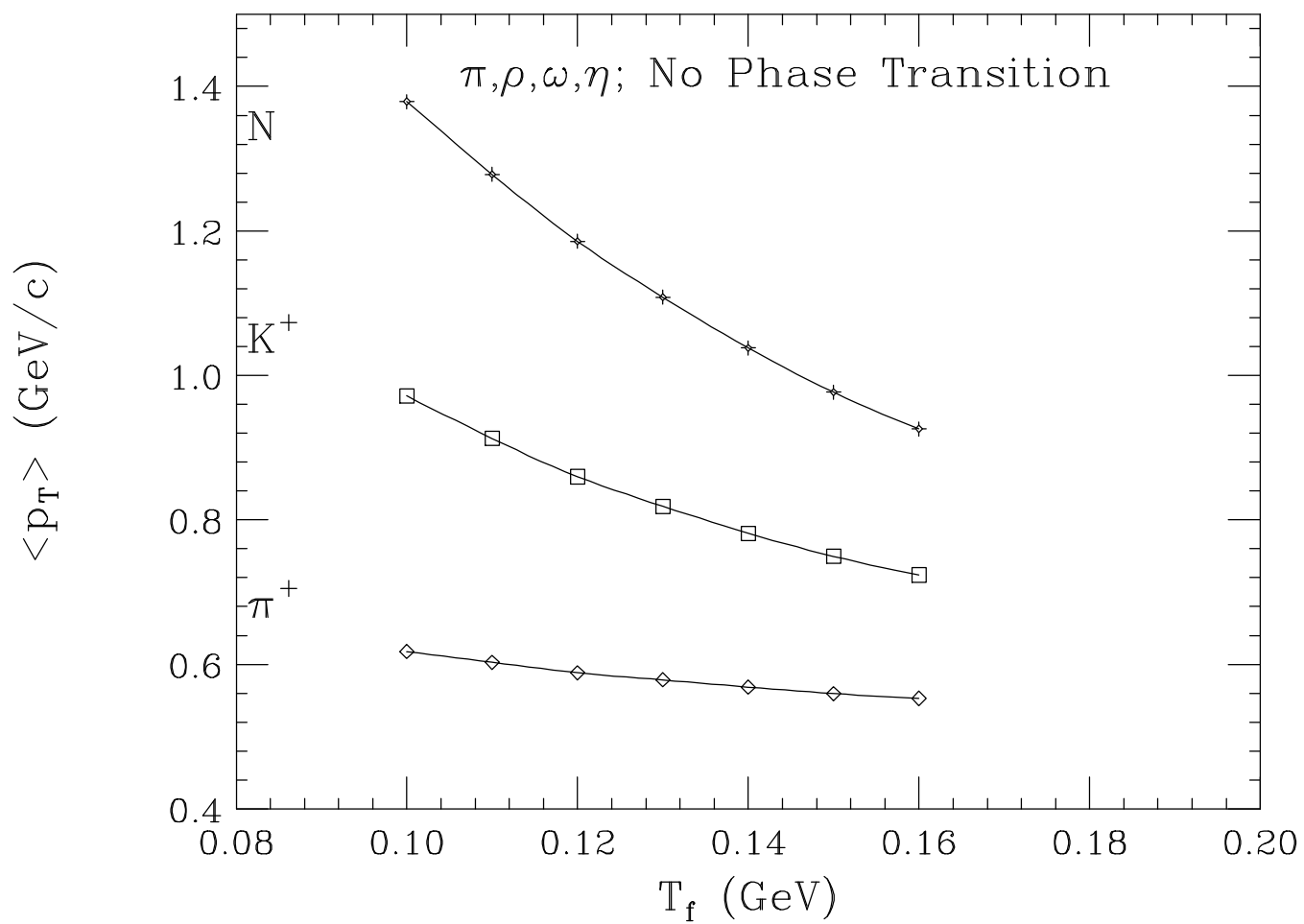


- FIG. 11a. Distribution in transverse mass at  $y=0$  of pions for a gas containing only  $\pi, \rho, \omega$  and  $\eta$  mesons. Different values of the freeze-out temperature are indicated. Phase transition occurs at  $T_c = 160$  MeV.
- FIG. 11b. Distribution in transverse mass at  $y=0$  of pions for a gas containing only  $\pi, \rho, \omega$  and  $\eta$  mesons. Different values of the freeze-out temperature are indicated.
- FIG. 12a. Distribution in transverse mass at  $y=0$  of pions for a gas containing all known resonances with masses below 2.5 GeV. Different values of the freeze-out temperature are indicated. The phase transition occurs at  $T_c = 160$  MeV.
- FIG. 12b. Distribution in transverse mass at  $y=0$  of pions for a gas containing all known resonances with masses below 2.5 GeV. Different values of the freeze-out temperature are indicated.
- FIG. 13a. Distribution in transverse mass at  $y=0$  of kaons for a gas containing only  $\pi, \rho, \omega$  and  $\eta$  mesons. Different values of the freeze-out temperature are indicated. Phase transition occurs at  $T_c = 160$  MeV.
- FIG. 13b. Distribution in transverse mass at  $y=0$  of kaons for a gas containing only  $\pi, \rho, \omega$  and  $\eta$  mesons. Different values of the freeze-out temperature are indicated.
- FIG. 14a. Distribution in transverse mass at  $y=0$  of kaons for a gas containing all known resonances with masses below 2.5 GeV. Different values of the freeze-out temperature are indicated. Phase transition occurs at  $T_c = 160$  MeV.
- FIG. 14b. Distribution in transverse mass at  $y=0$  of kaons for a gas containing all known resonances with masses below 2.5 GeV. Different values of the freeze-out temperature are indicated.
- FIG. 15a. Average transverse momentum of  $\pi^+, K^+$  and nucleons as a function of the freeze-out temperature  $T_f$  for a gas containing all resonances with masses up to 2.5 GeV. No phase transition takes place.
- FIG. 15b. Average transverse momentum of  $\pi^+, K^+$  and nucleons as a function of the freeze-out temperature  $T_f$  for a gas containing all resonances with masses up to 2.5 GeV. A phase transition has been built in at  $T_c = 160$  MeV.
- FIG. 16. Distribution in transverse momentum at  $y=0$  of photons for a gas containing only  $\pi, \rho, \omega$  and  $\eta$  mesons with (dashed line) and without (full line) phase transition.
- FIG. 17. Distribution in transverse momentum at  $y=0$  of photons for a gas containing all known resonances with masses below 2.5 GeV with (dashed line) and without (full line) phase transition.
- FIG. 18a. The  $\eta/\pi$  ratio as a function of the transverse momentum  $p_T$  for a gas containing only  $\pi, \rho, \omega$  and  $\eta$  mesons. Different values of the freeze-out temperature are indicated.
- FIG. 18b. The  $\eta/\pi$  ratio as a function of the transverse momentum  $p_T$  for a gas containing only  $\pi, \rho, \omega$  and  $\eta$  mesons. Different values of the freeze-out temperature are indicated.
- FIG. 19a. The  $\eta/\pi$  ratio as a function of the transverse momentum  $p_T$  for a gas containing all known resonances with masses below 2.5 GeV. Different values of the freeze-out temperature are indicated.
- FIG. 19b. The  $\eta/\pi$  ratio as a function of the transverse momentum  $p_T$  a gas containing all known resonances with masses below 2.5 GeV. Different values of the freeze-out temperature are indicated.

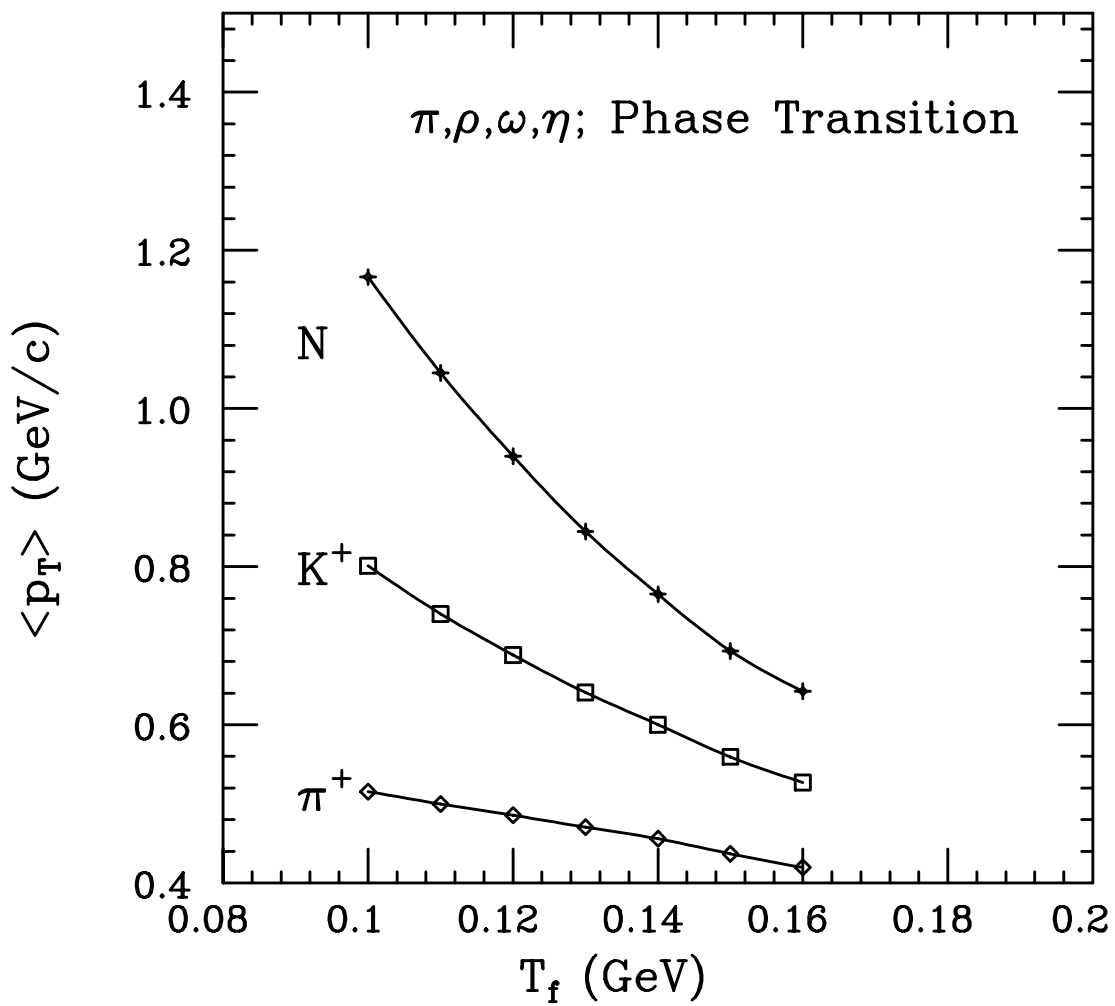
### Average $p_T$ of Hadrons



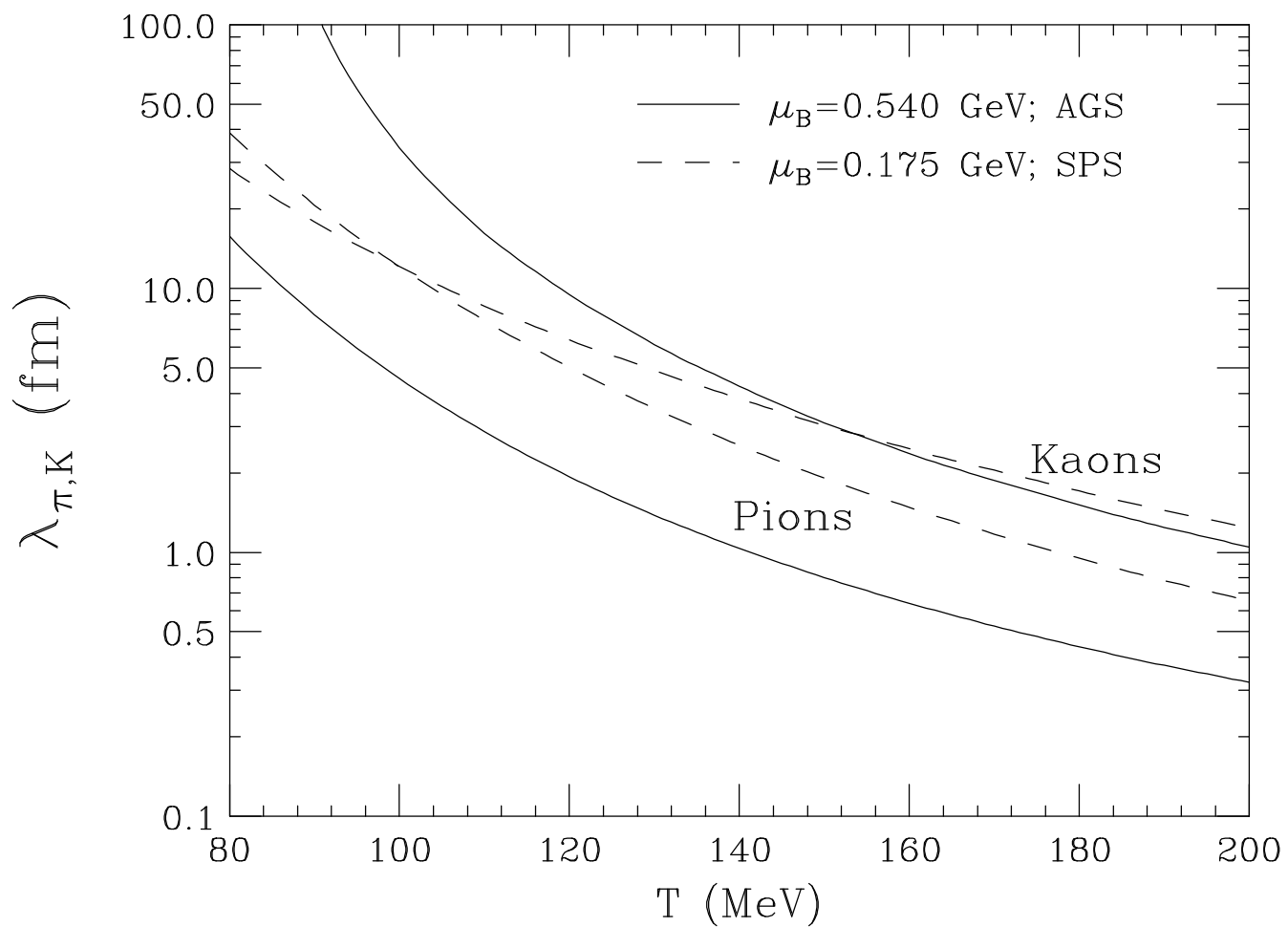
### Average $p_T$ of Hadrons



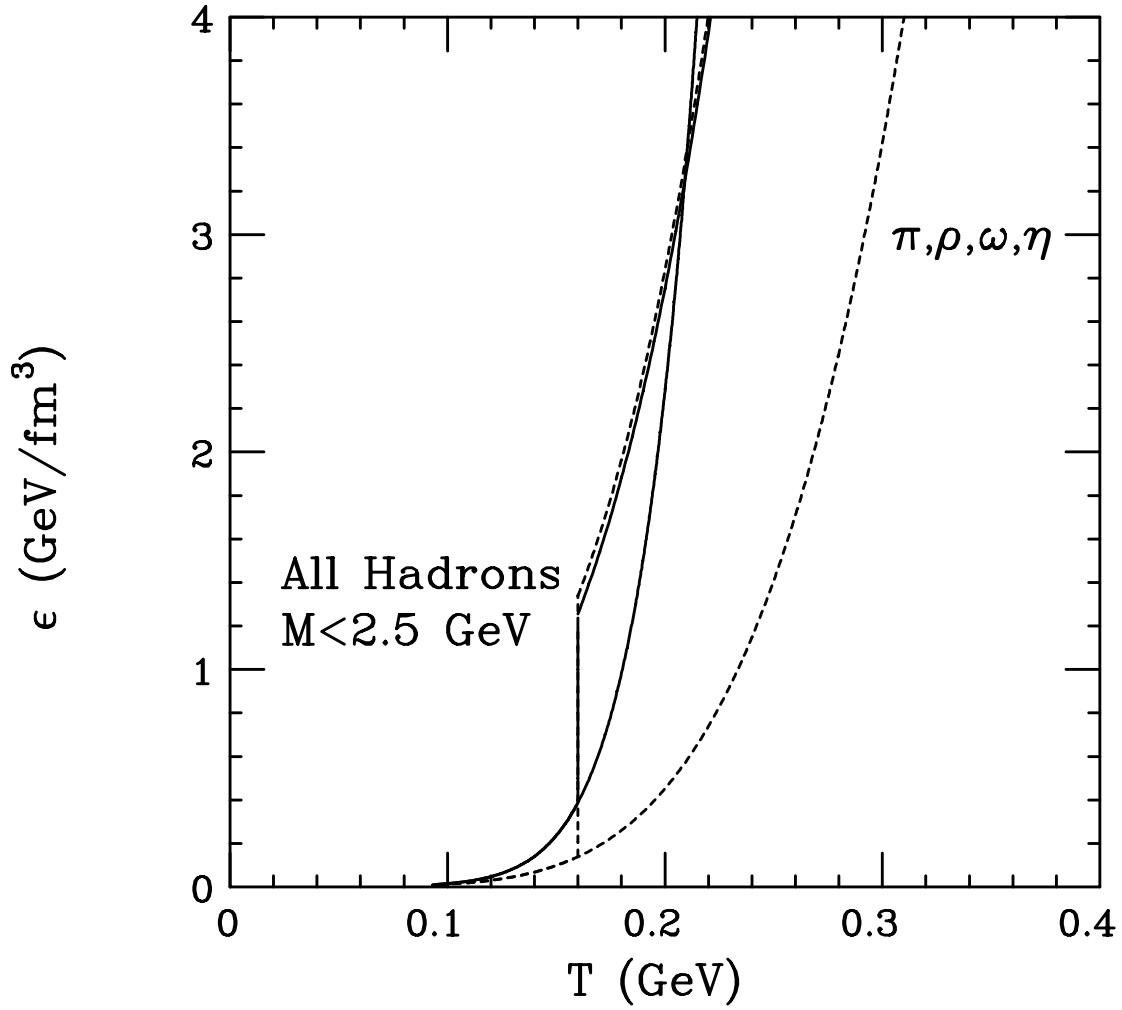
### Average $p_T$ of Hadrons



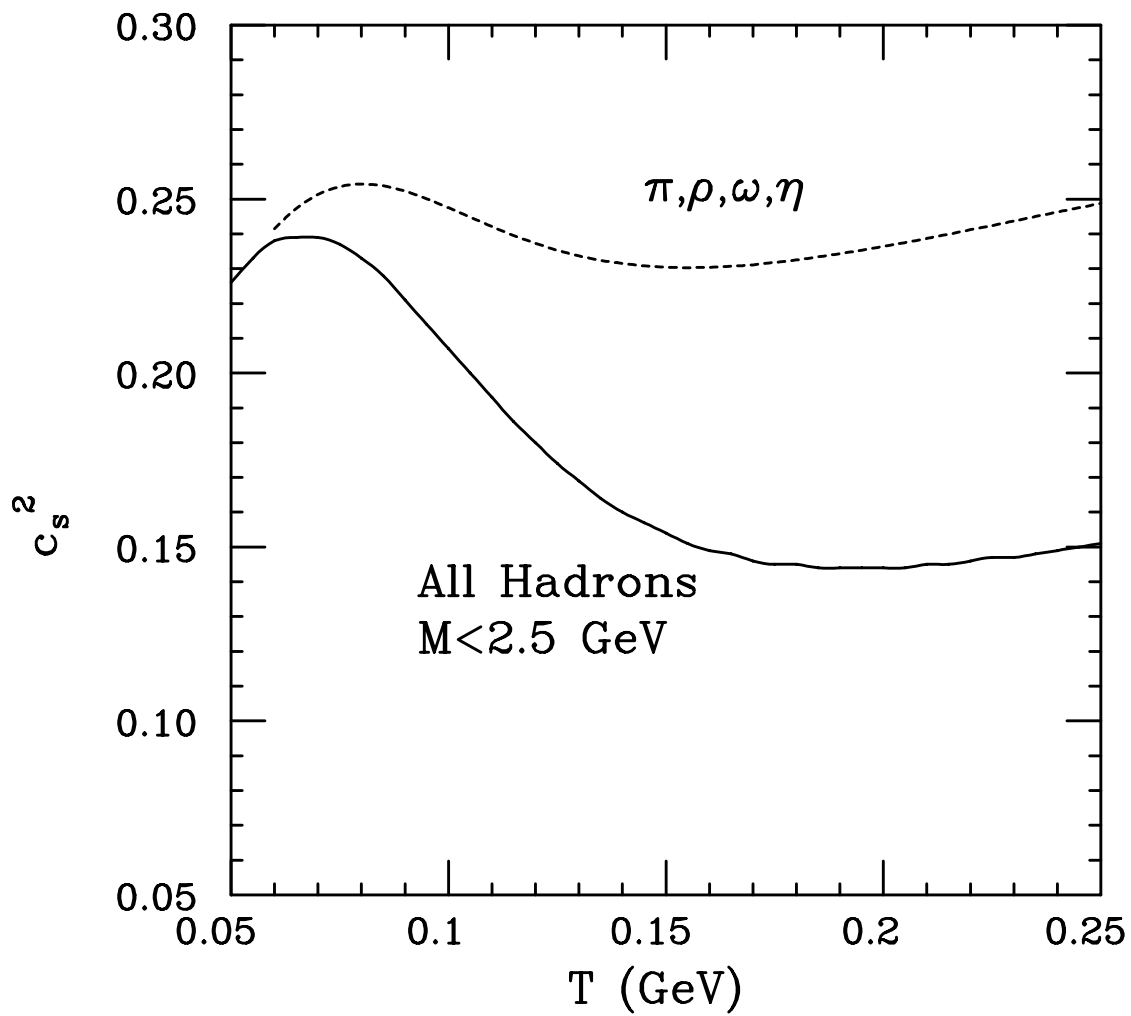
Mean Free Paths of Pions and Kaons



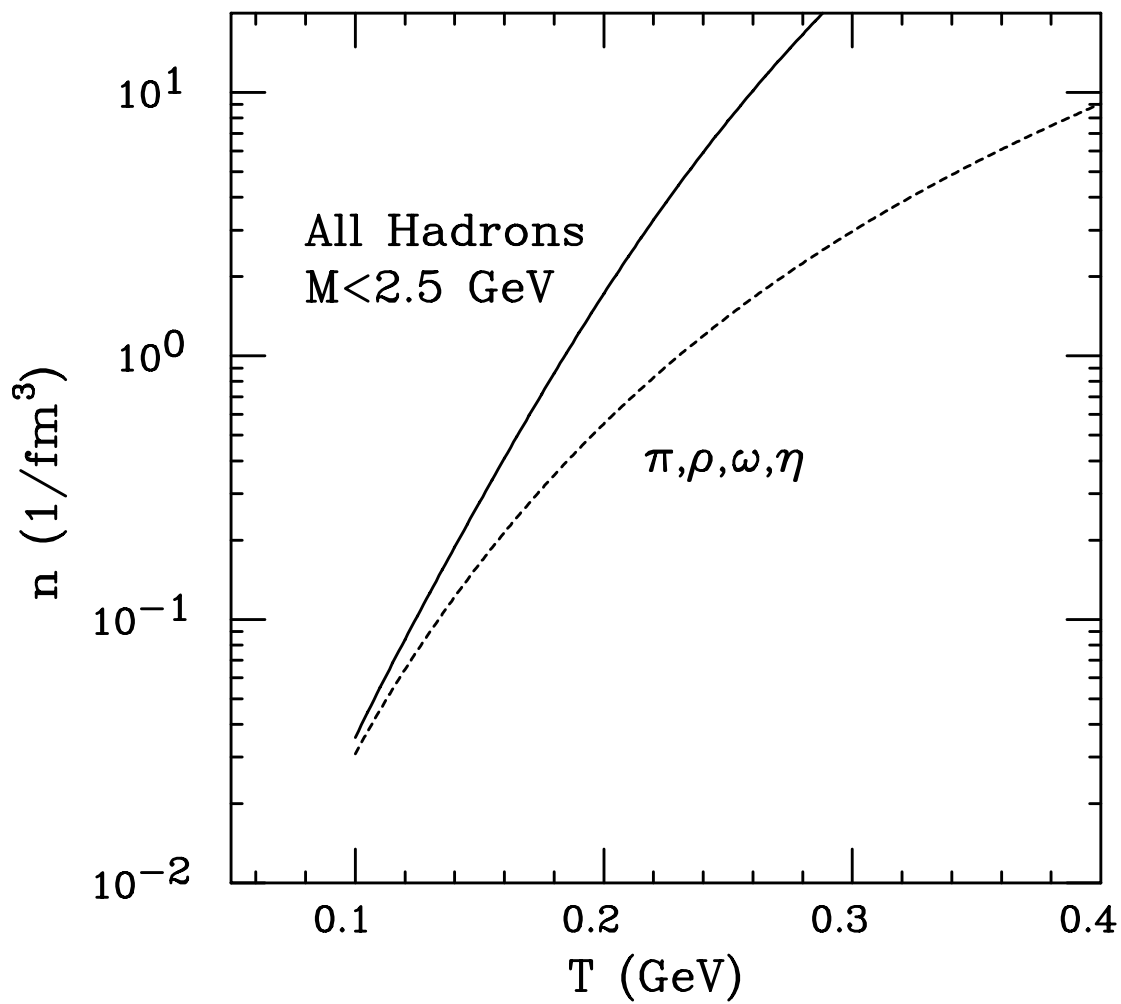
# Energy Density



### Square of Speed of Sound

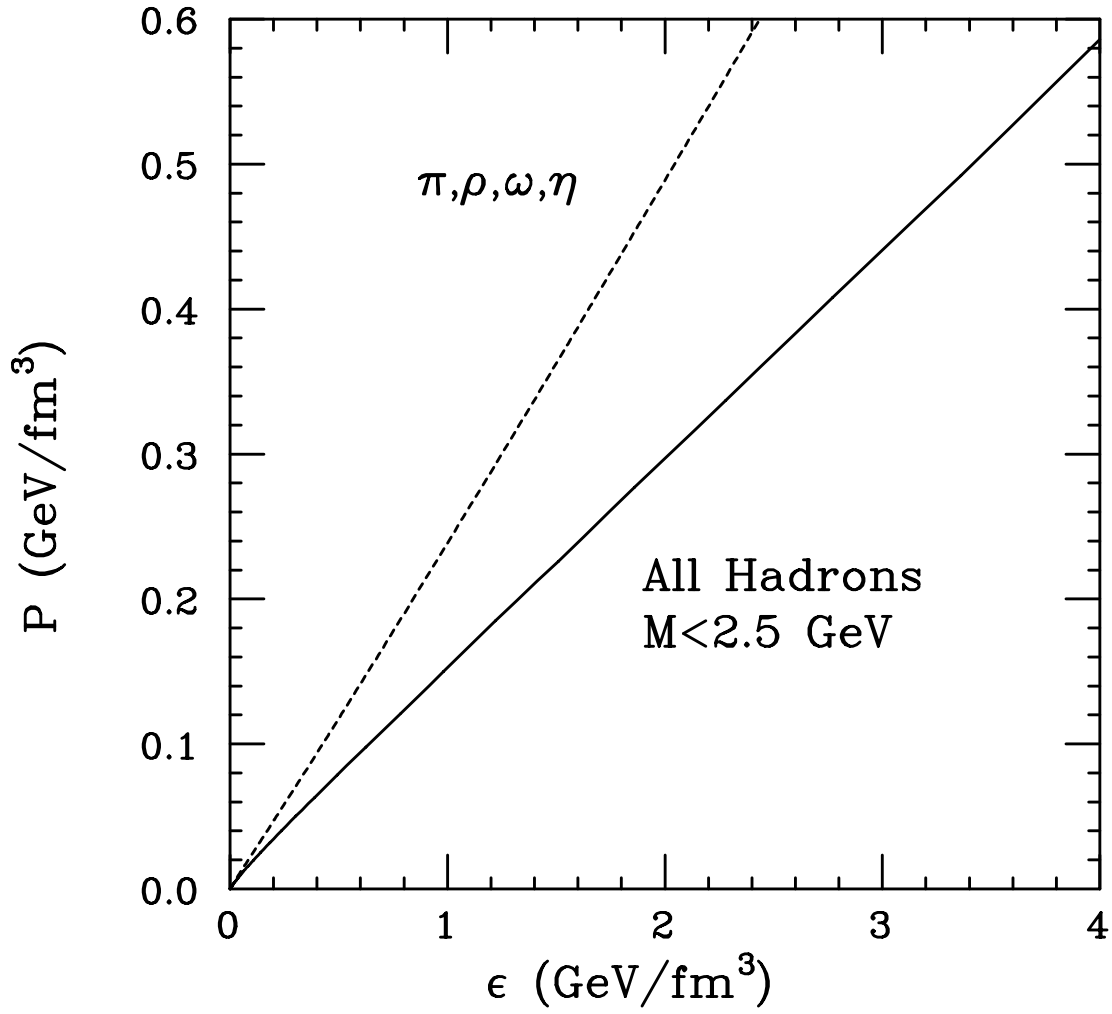


# Density of Hadrons

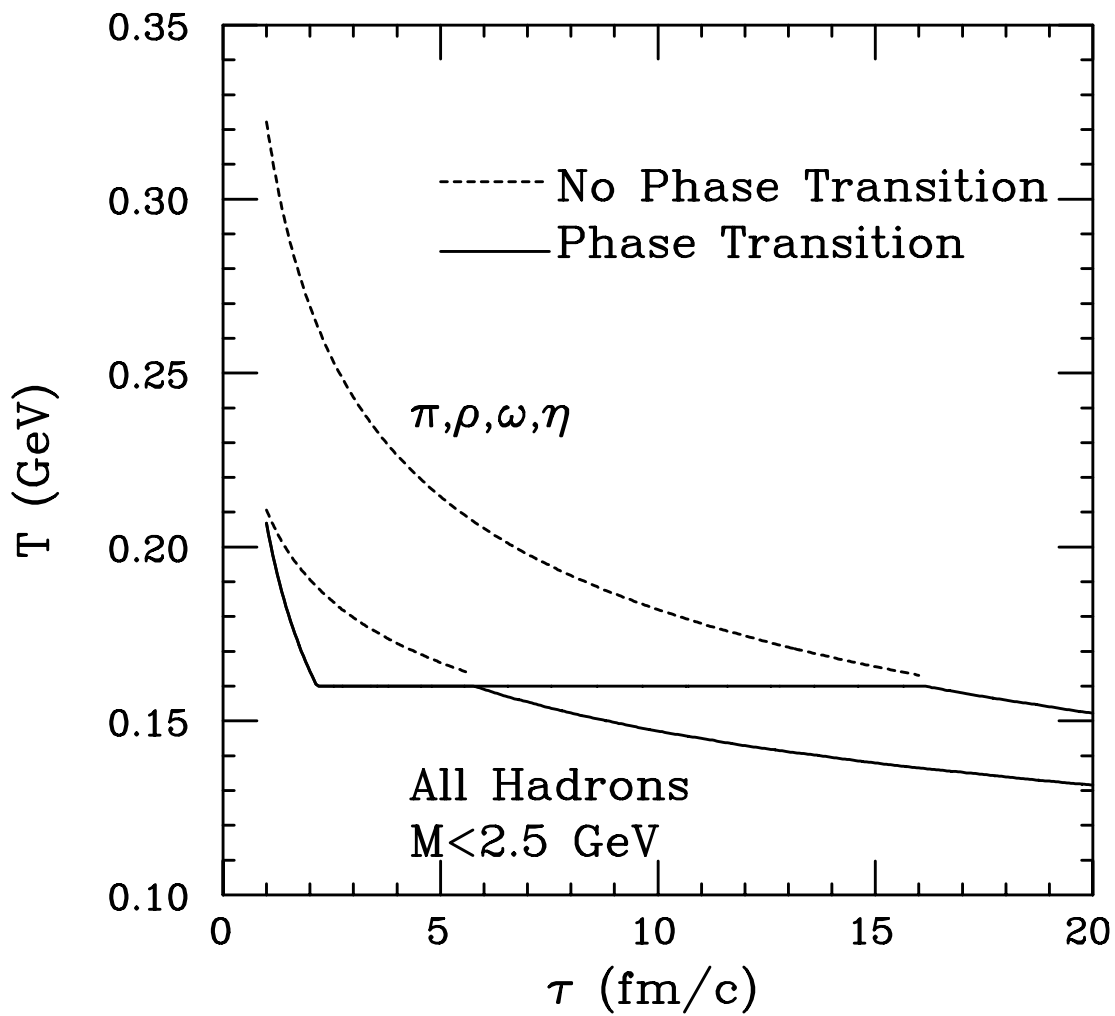




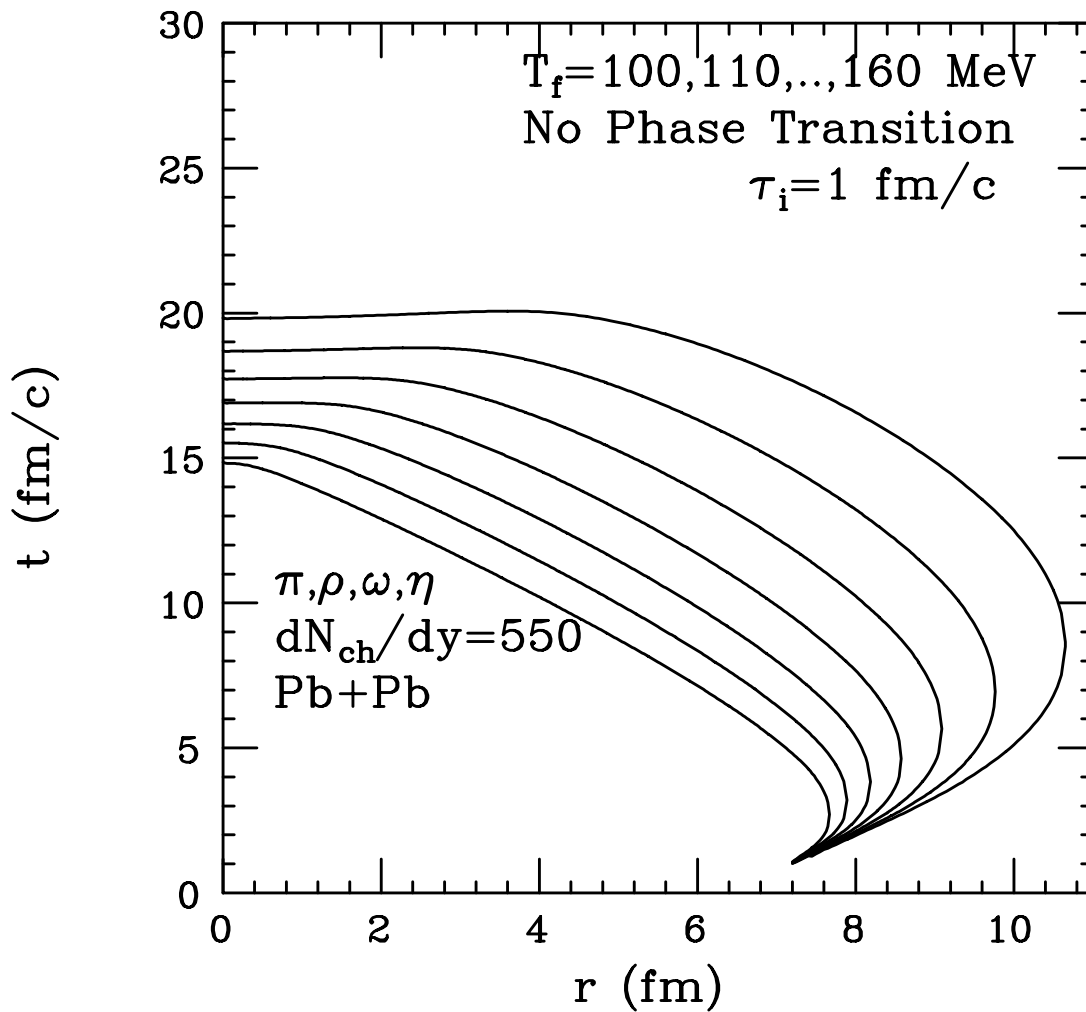
### Equation of State



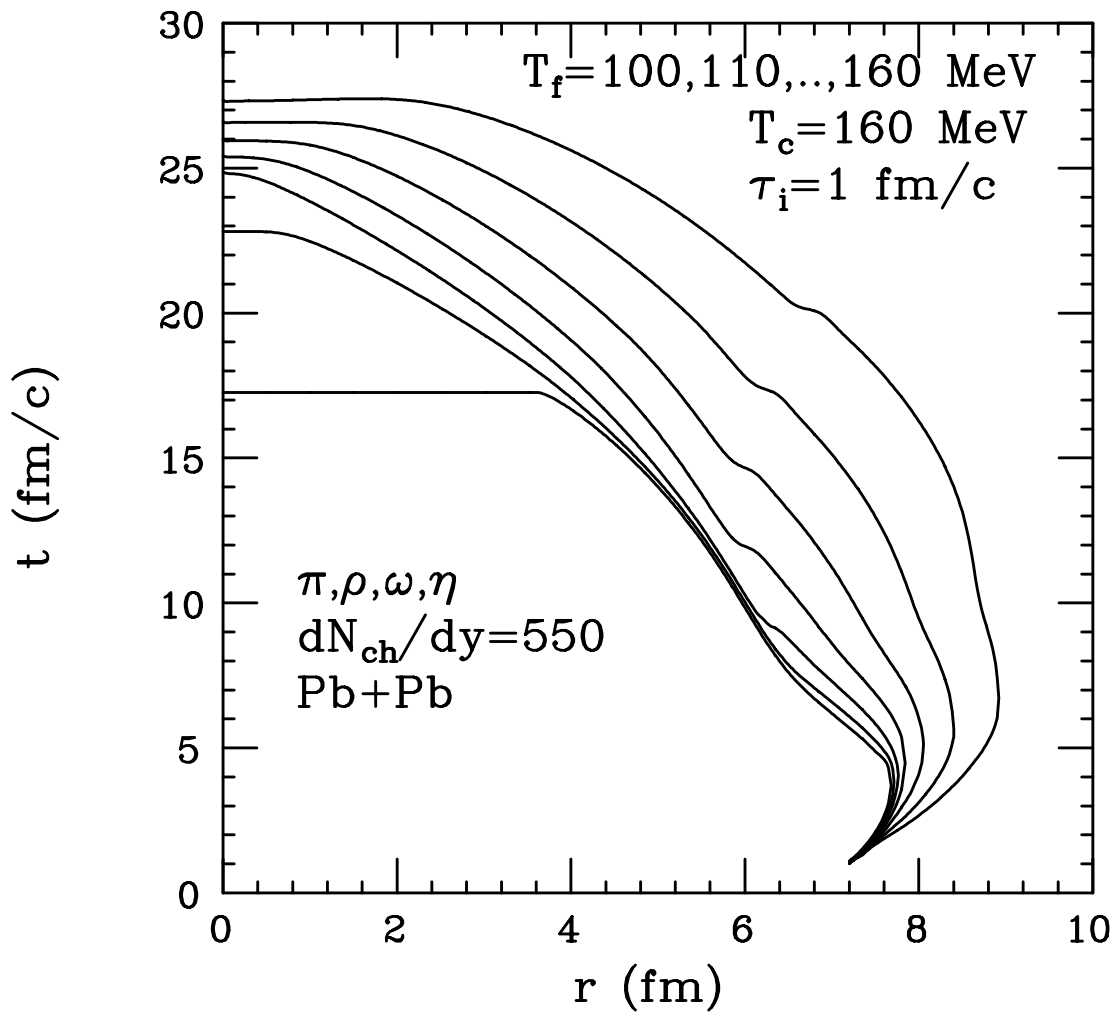
# Bjorken Hydrodynamics



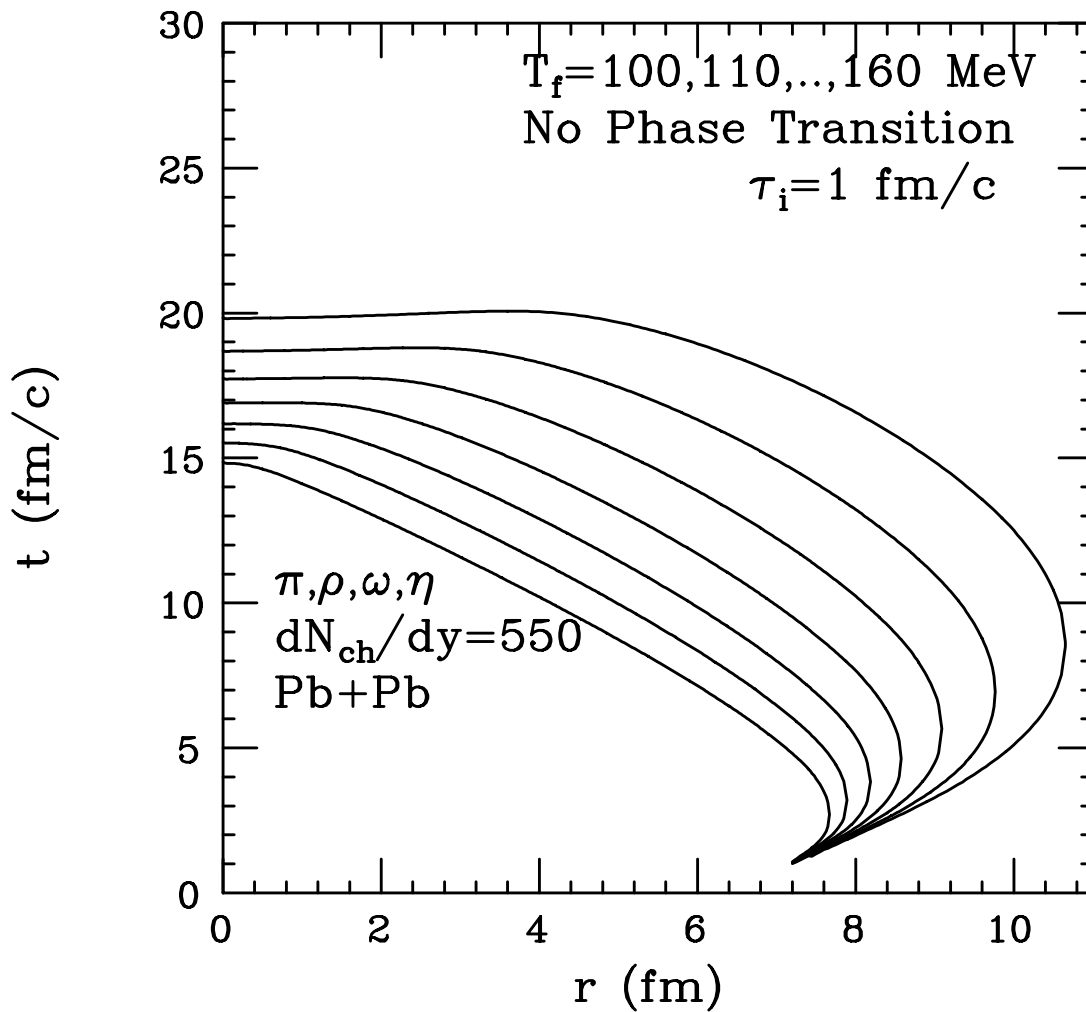
### Freeze-out Surface at $z=0$



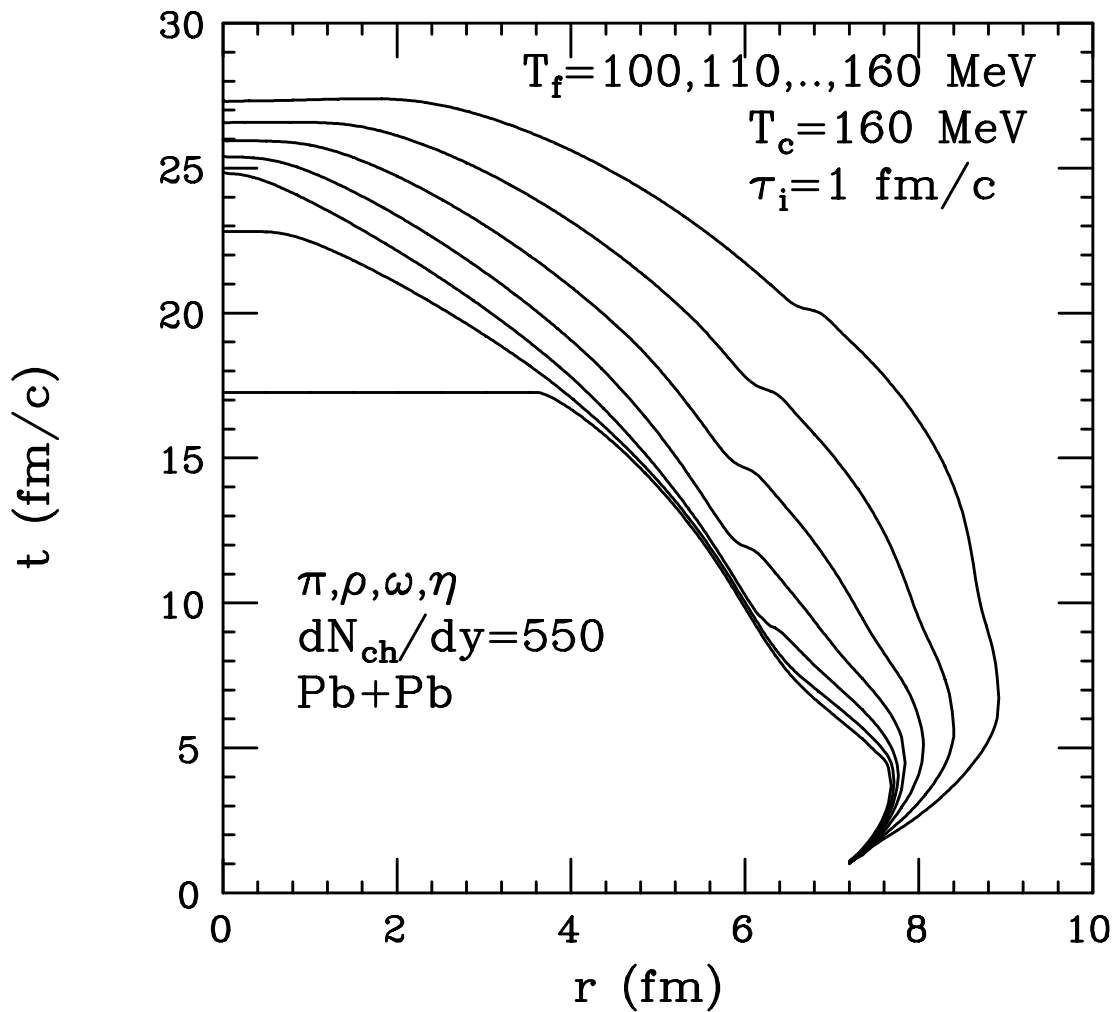
### Freeze-out Surface at $z=0$



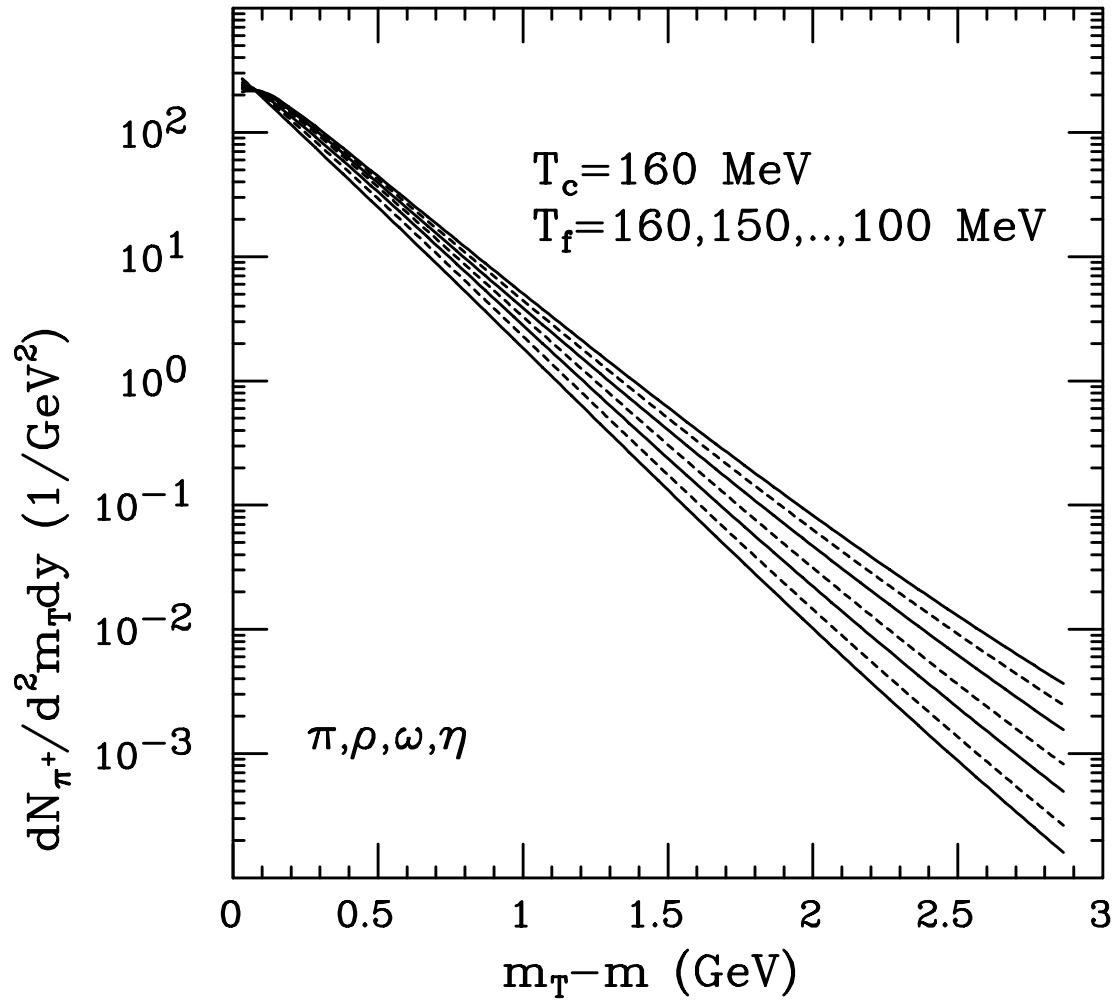
### Freeze-out Surface at $z=0$



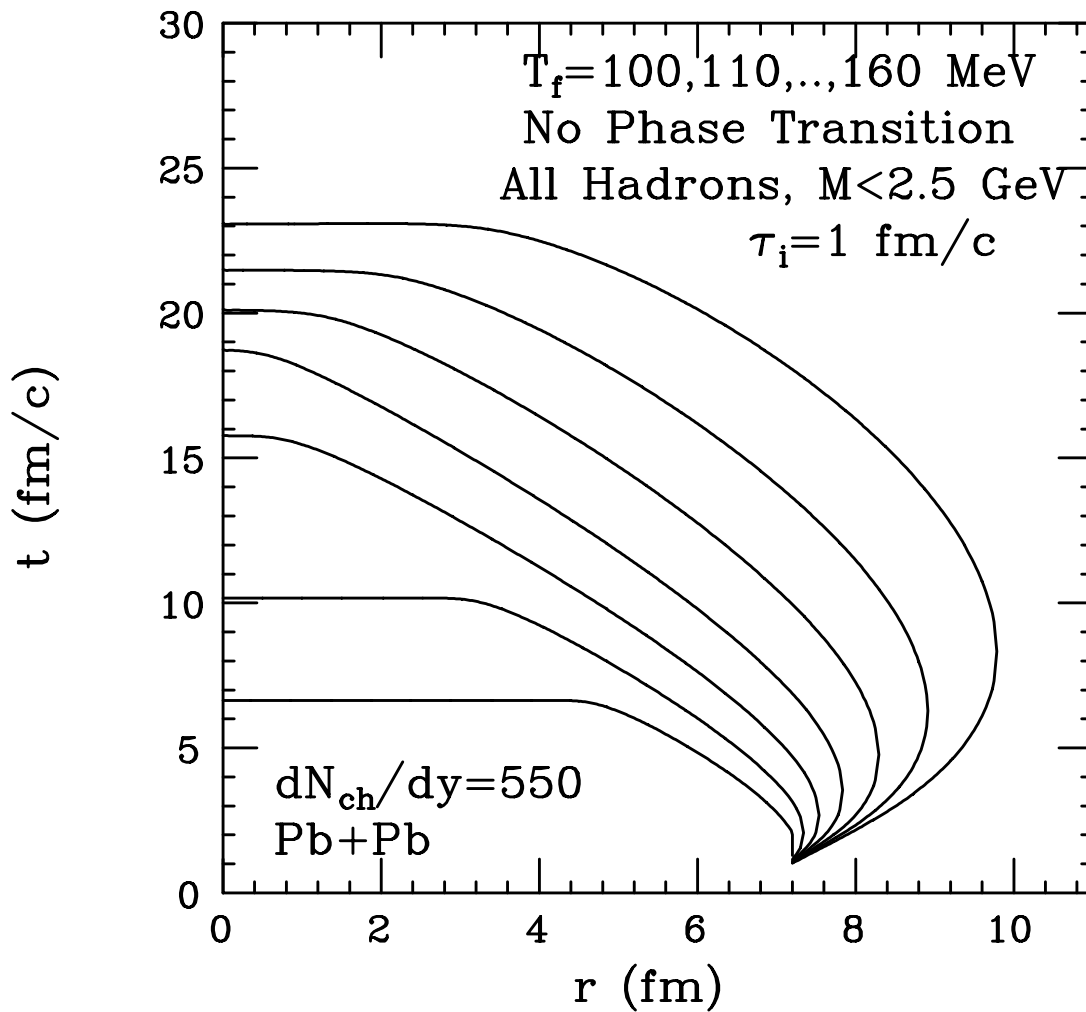
### Freeze-out Surface at $z=0$



# Distribution of $\pi^+$

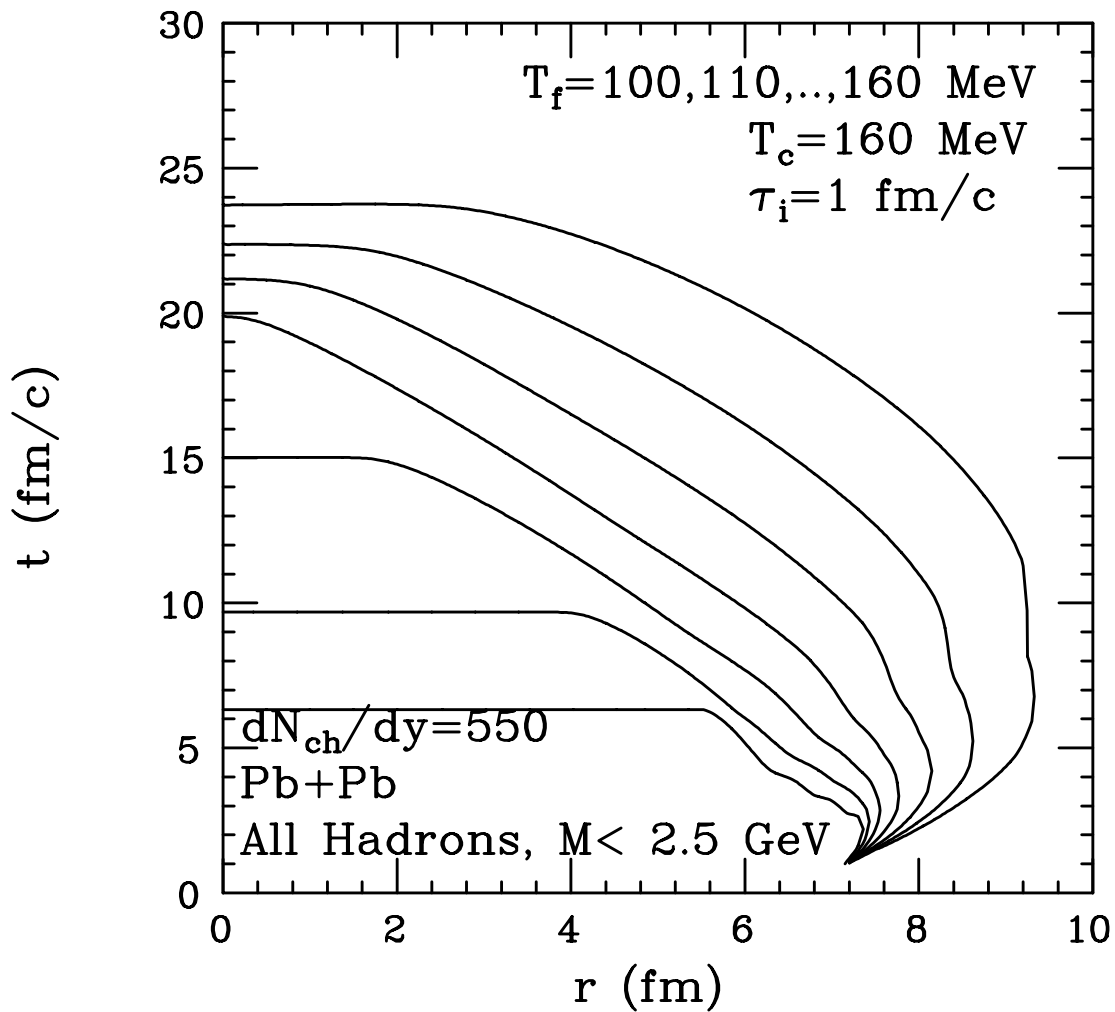


Freeze-out Surface at  $z=0$

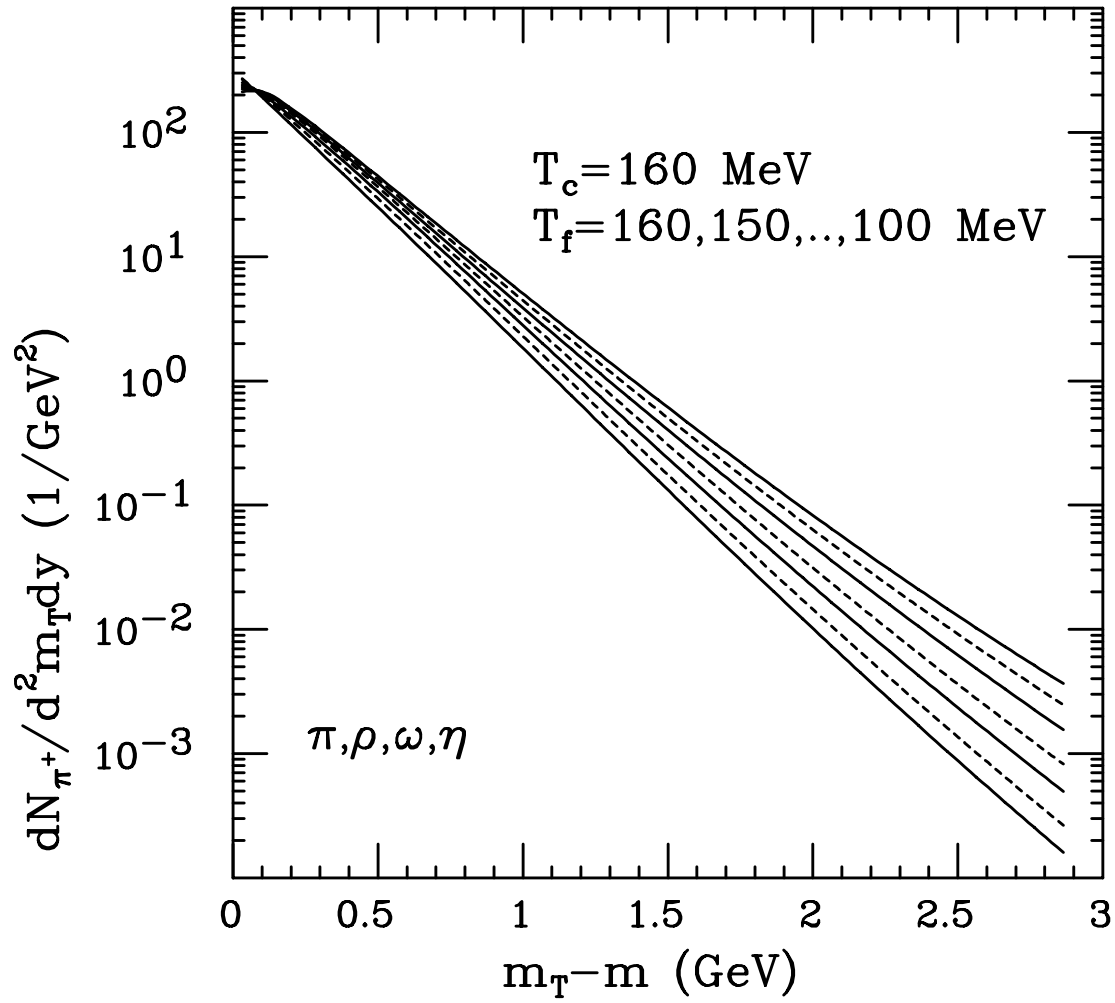




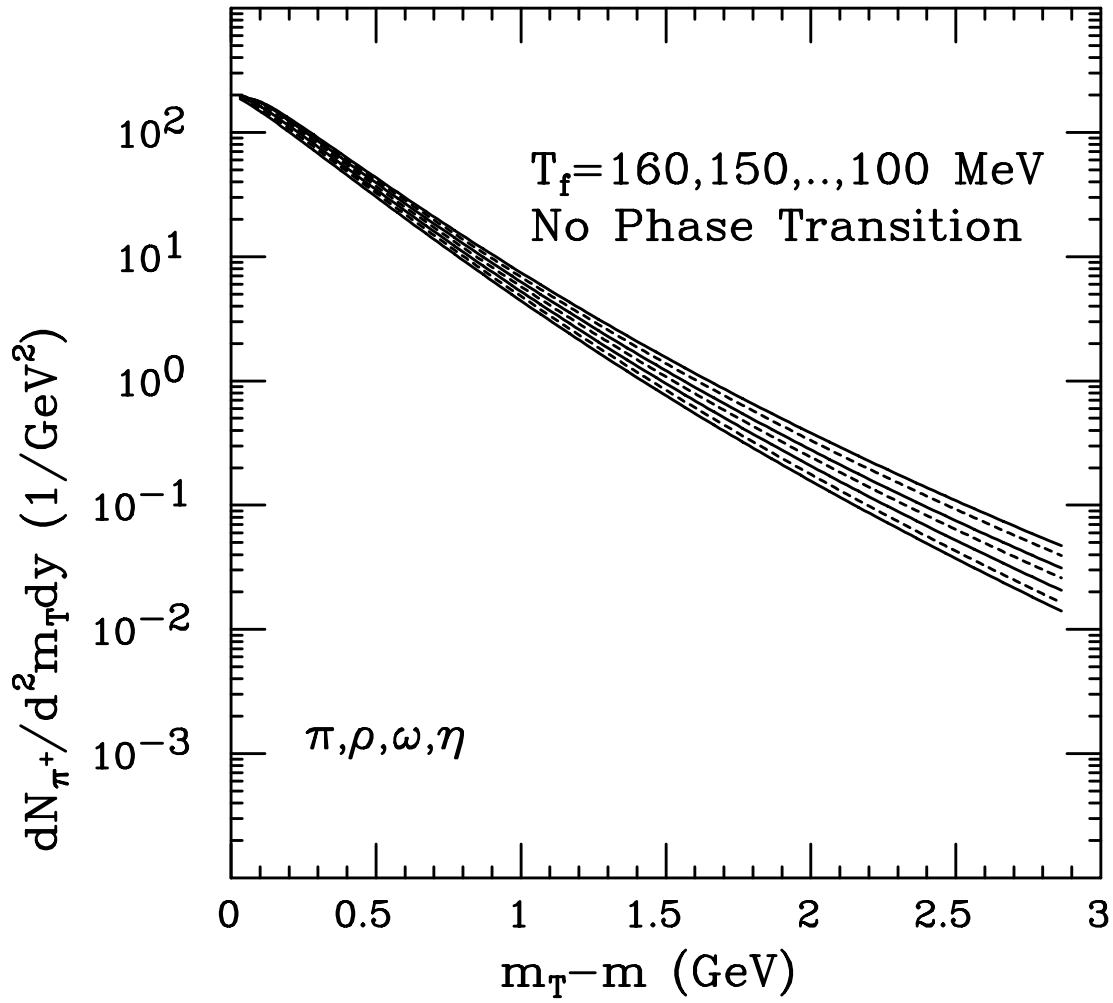
### Freeze-out Surface at $z=0$



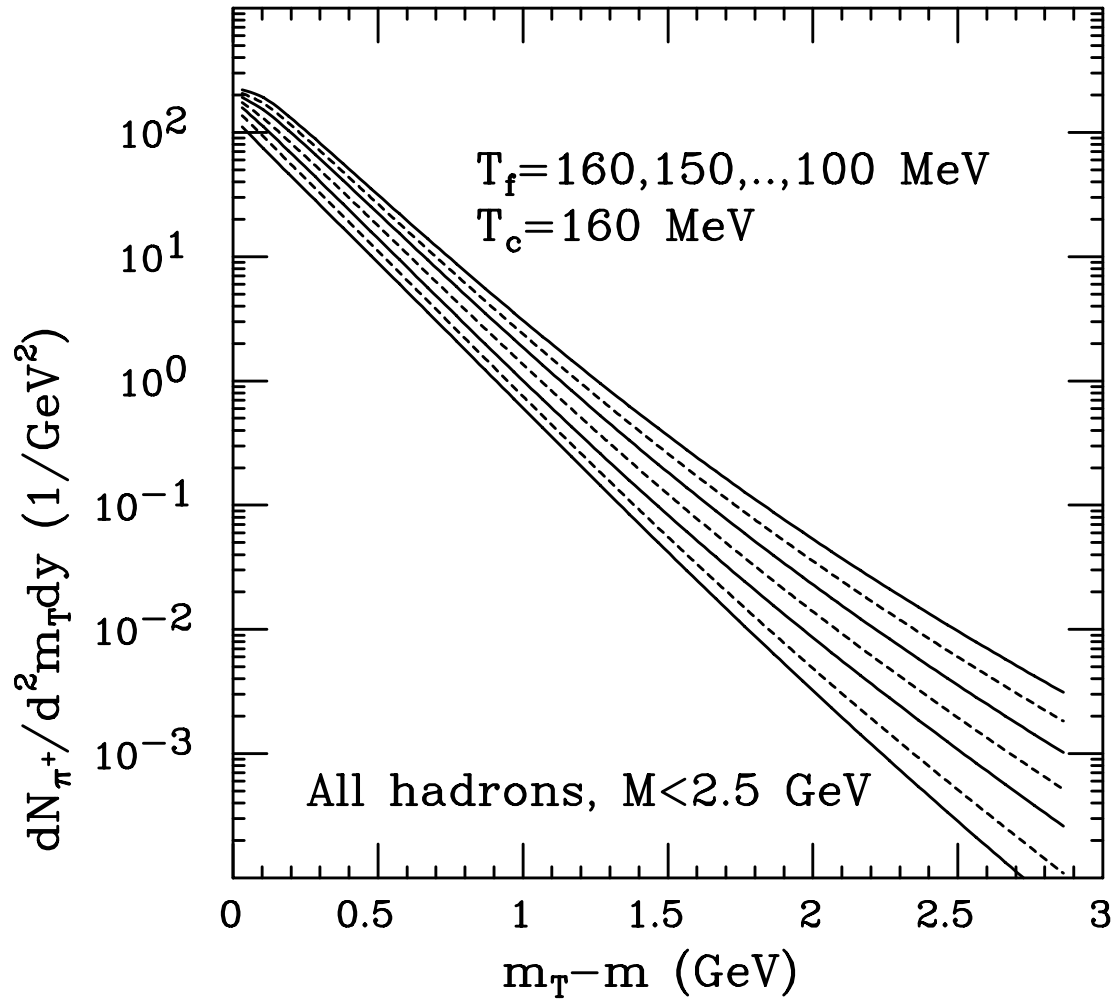
# Distribution of $\pi^+$



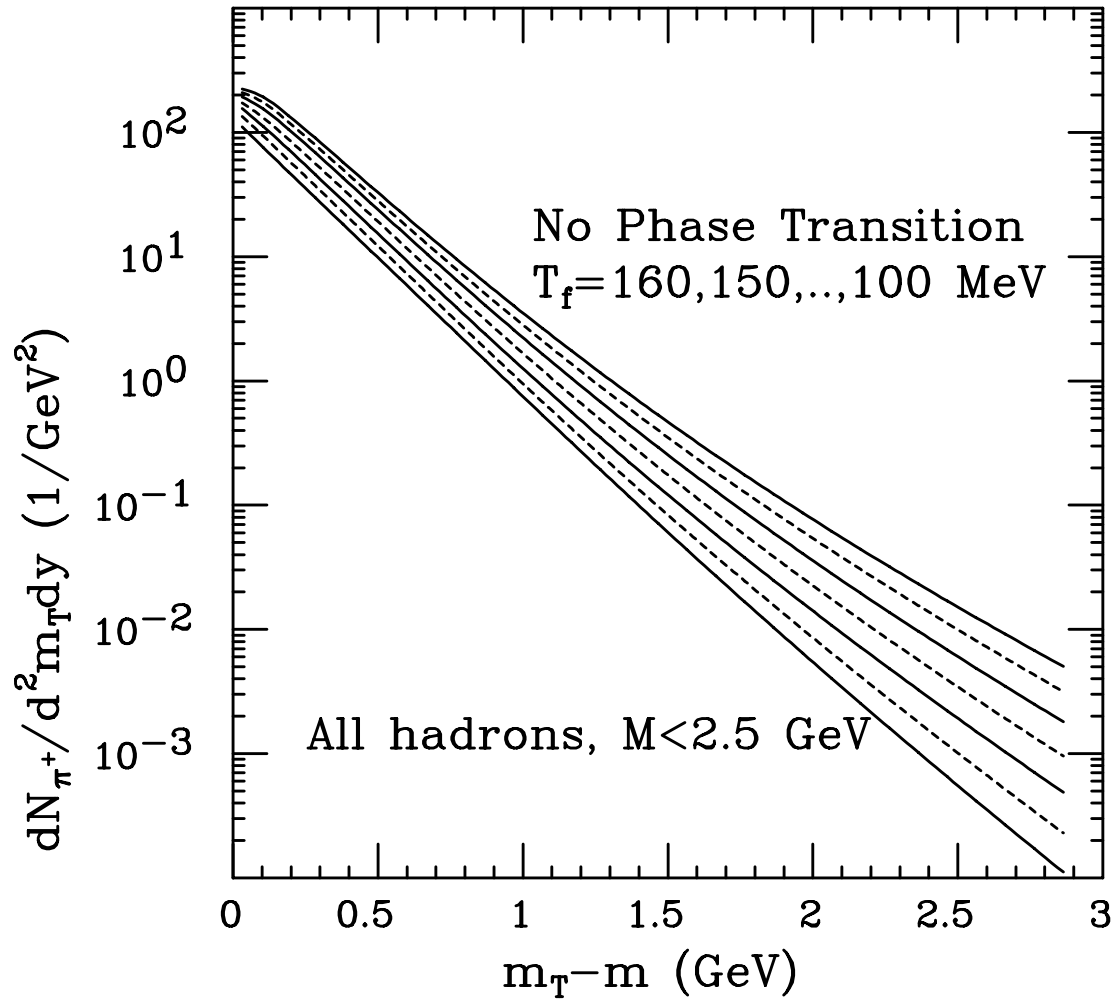
# Distribution of $\pi^+$



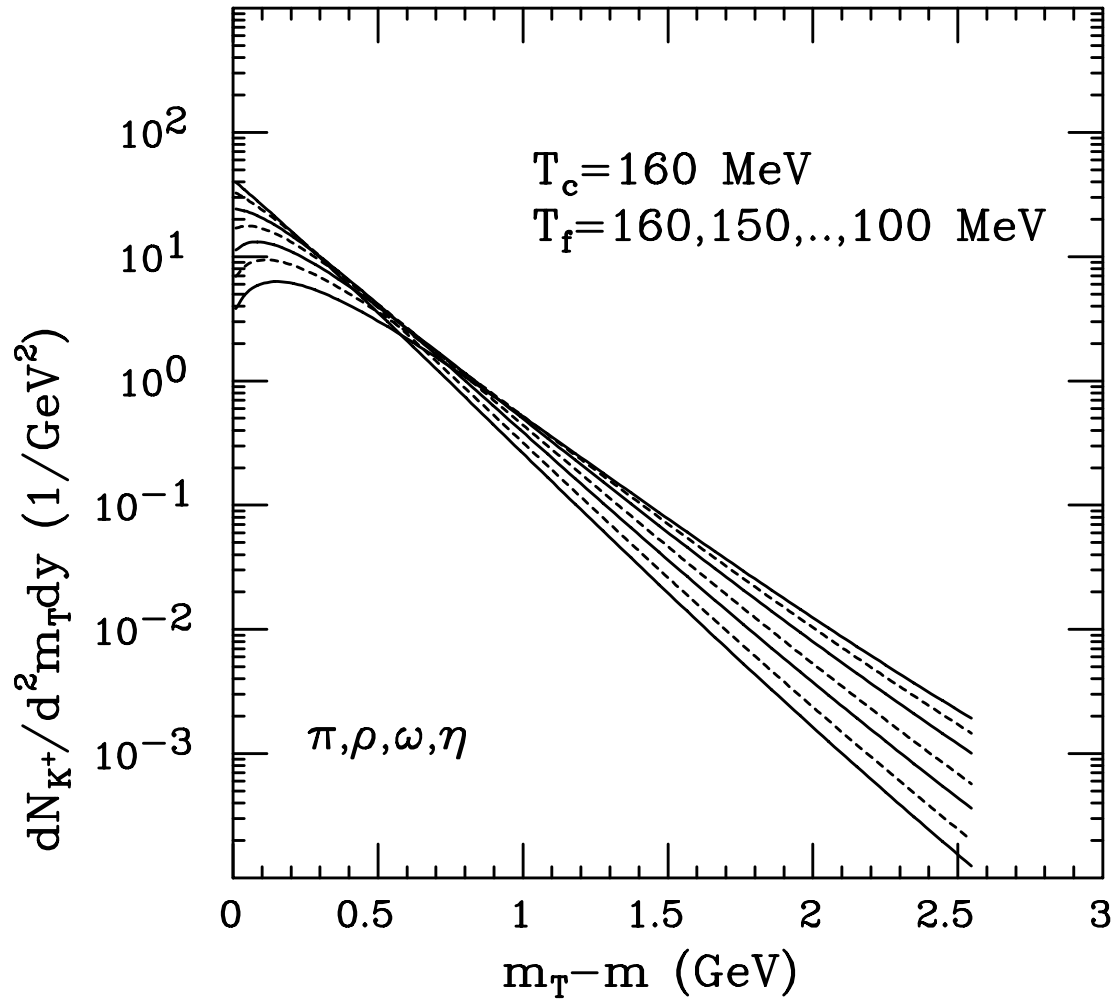
# Distribution of $\pi^+$



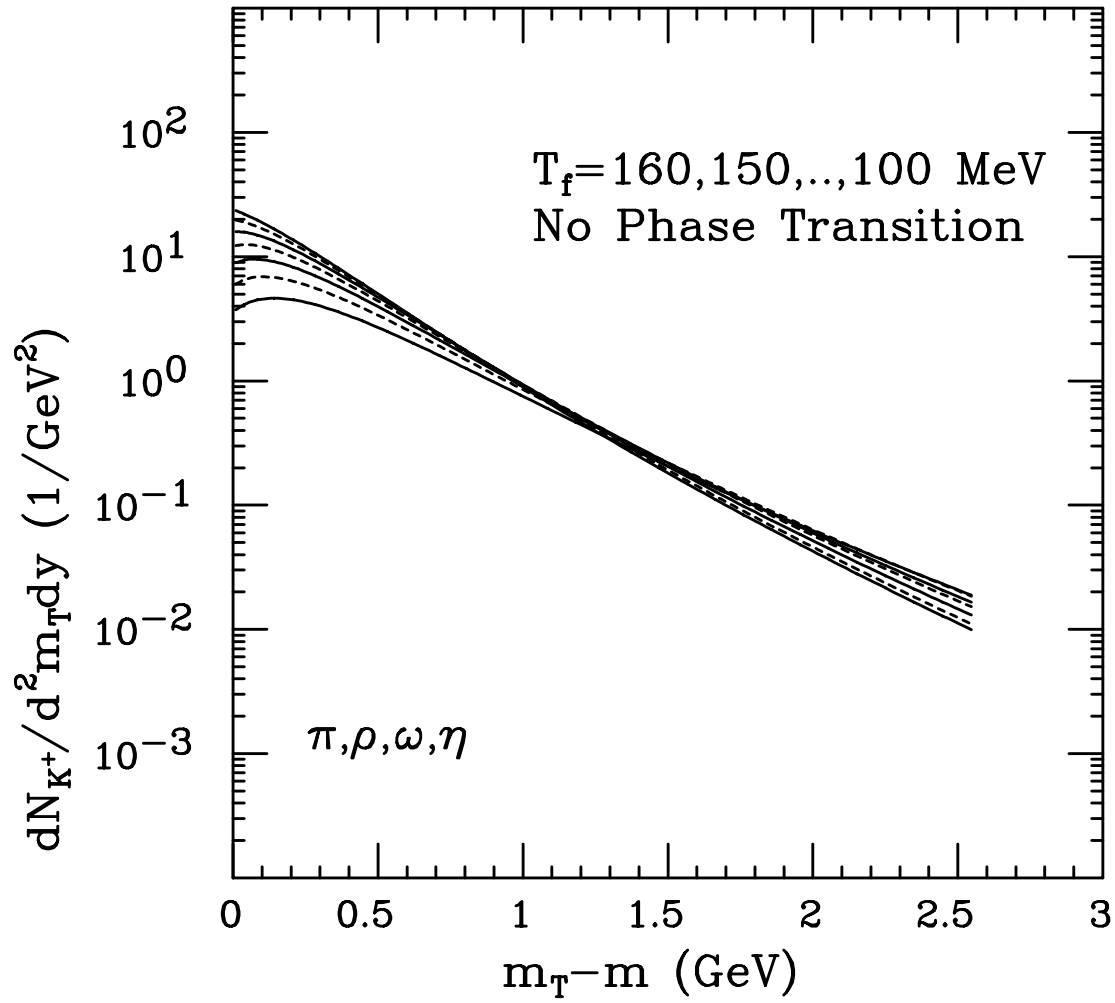
# Distribution of $\pi^+$



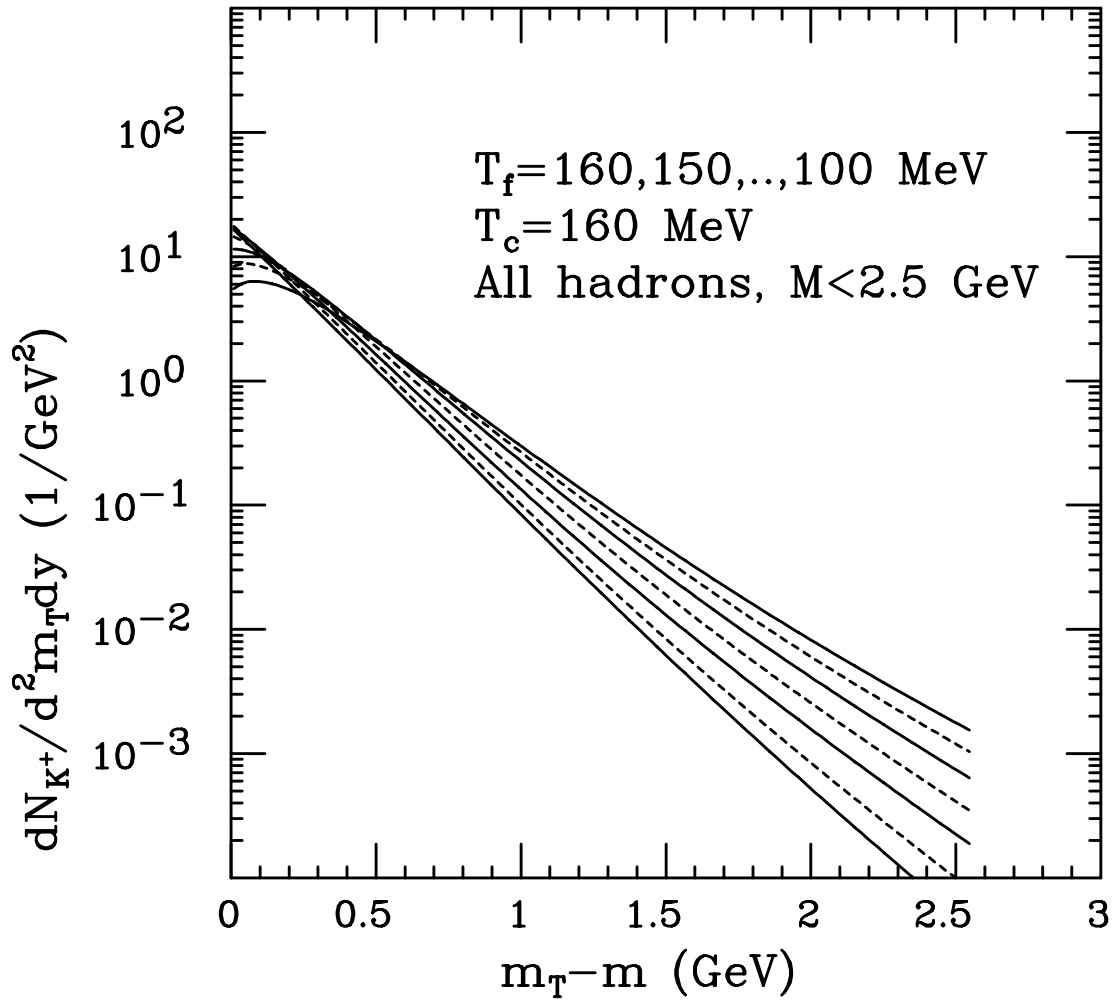
# Distribution of $K^+$



# Distribution of $K^+$

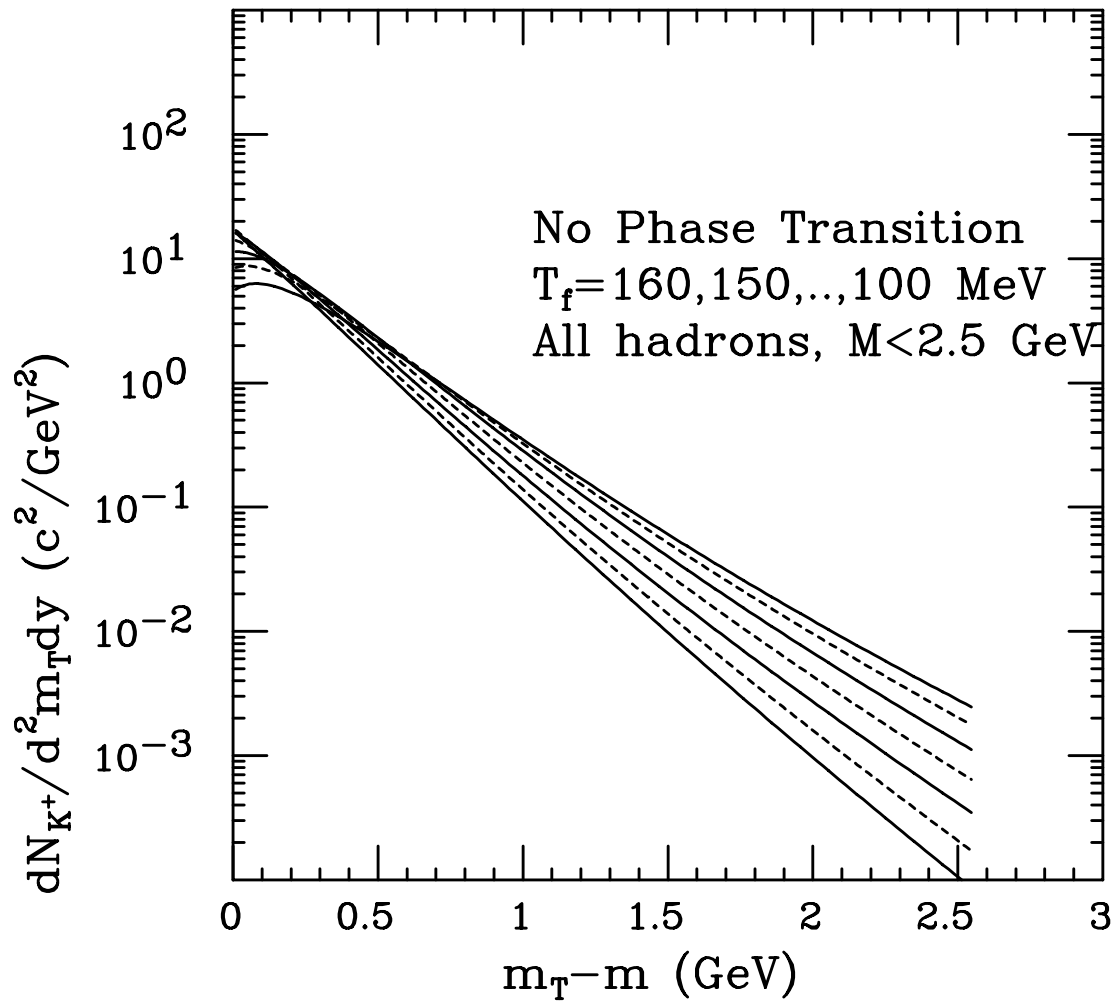


# Distribution of $K^+$

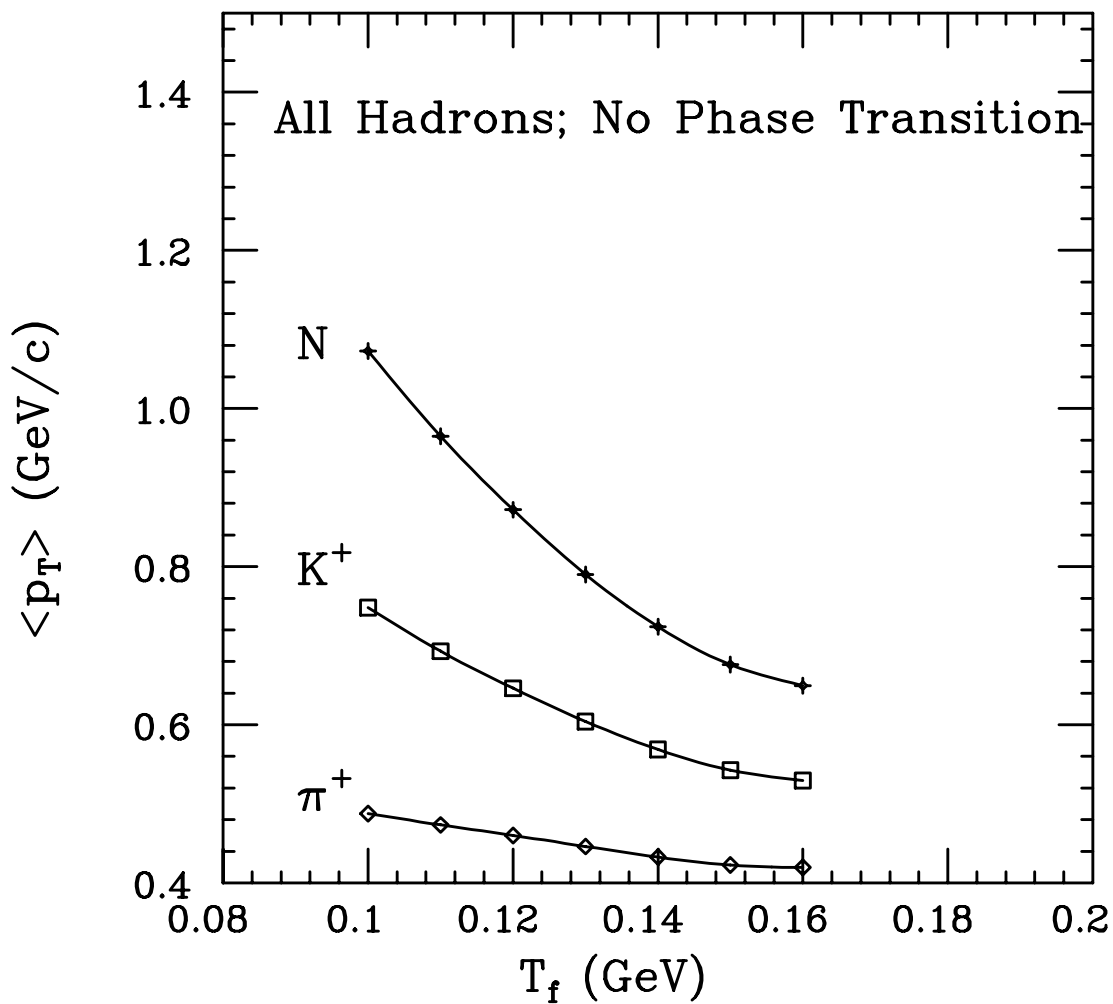




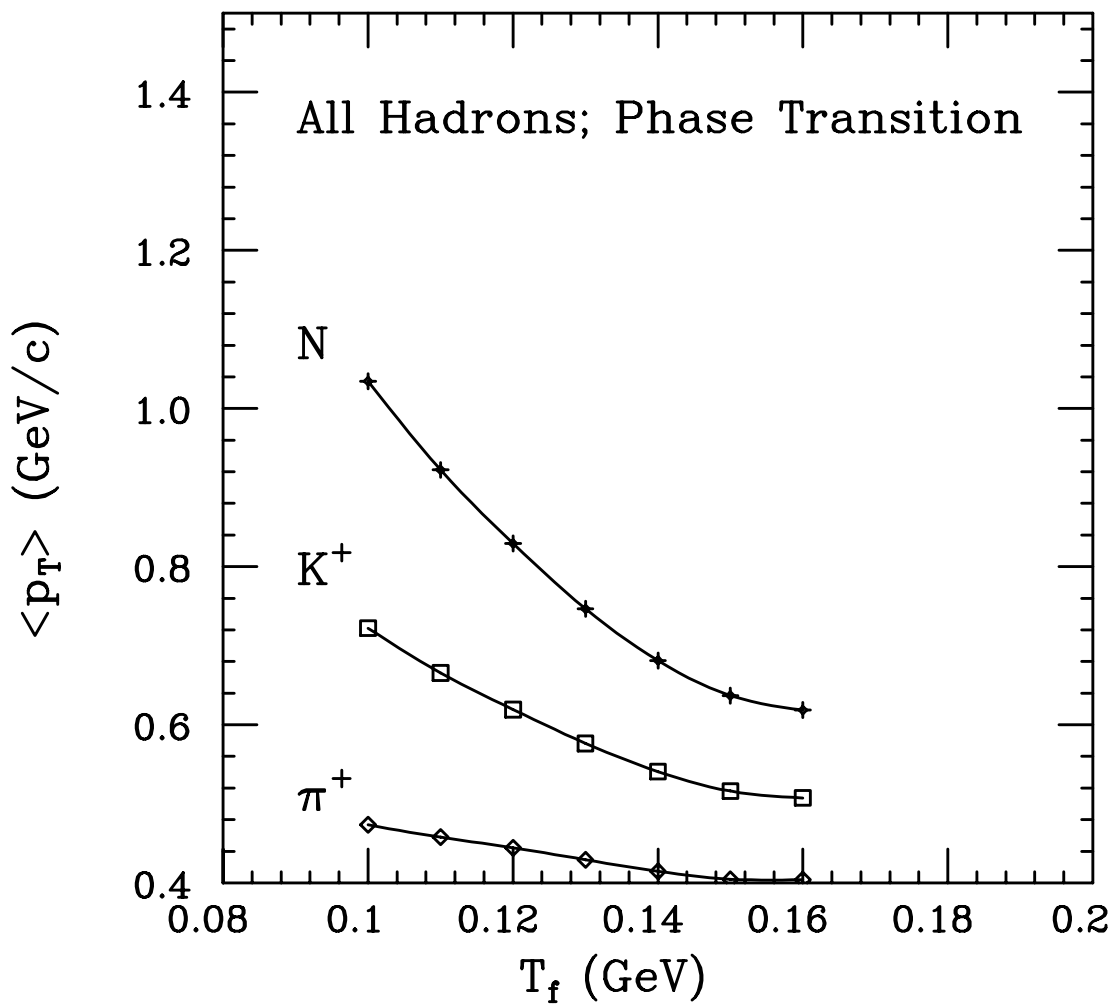
# Distribution of $K^+$



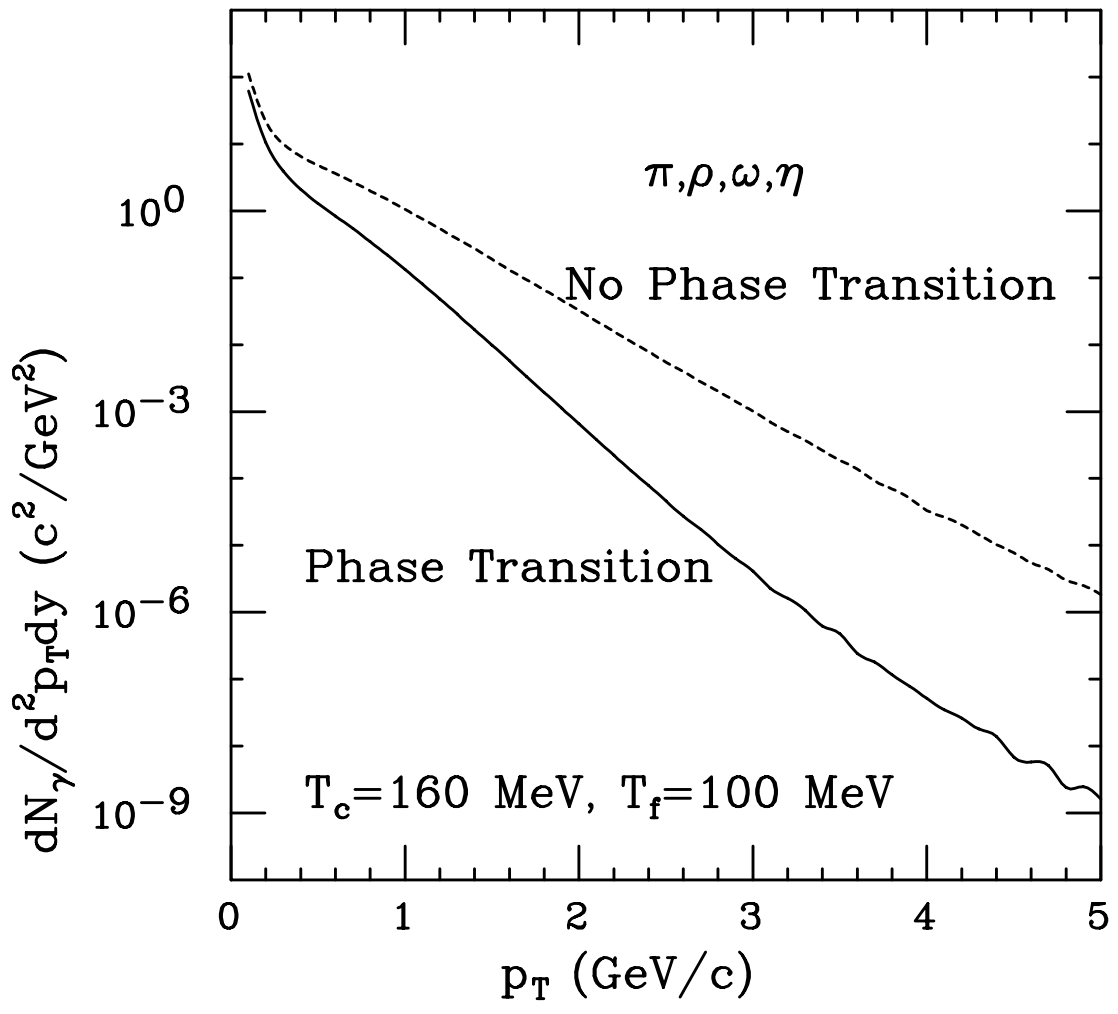
### Average $p_T$ of Hadrons



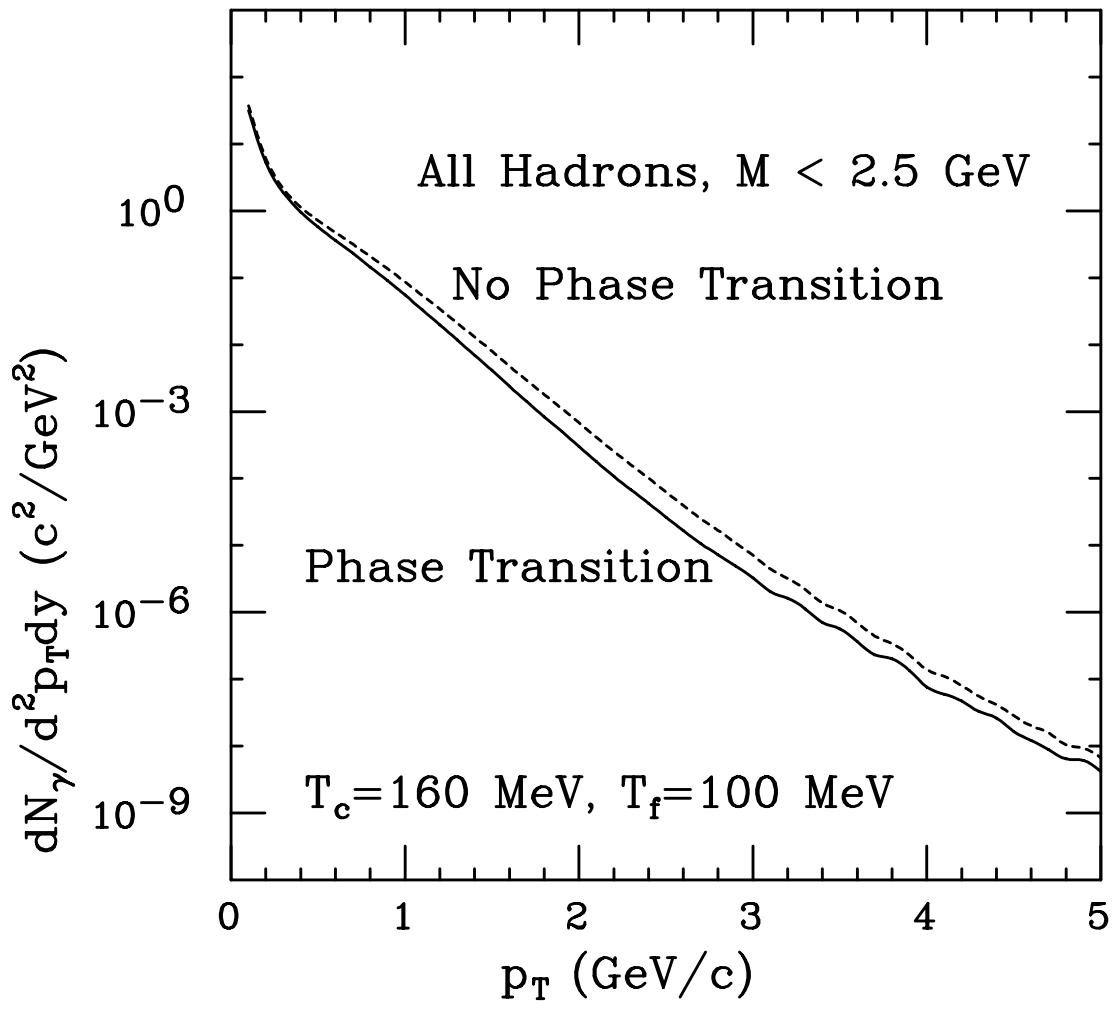
### Average $p_T$ of Hadrons



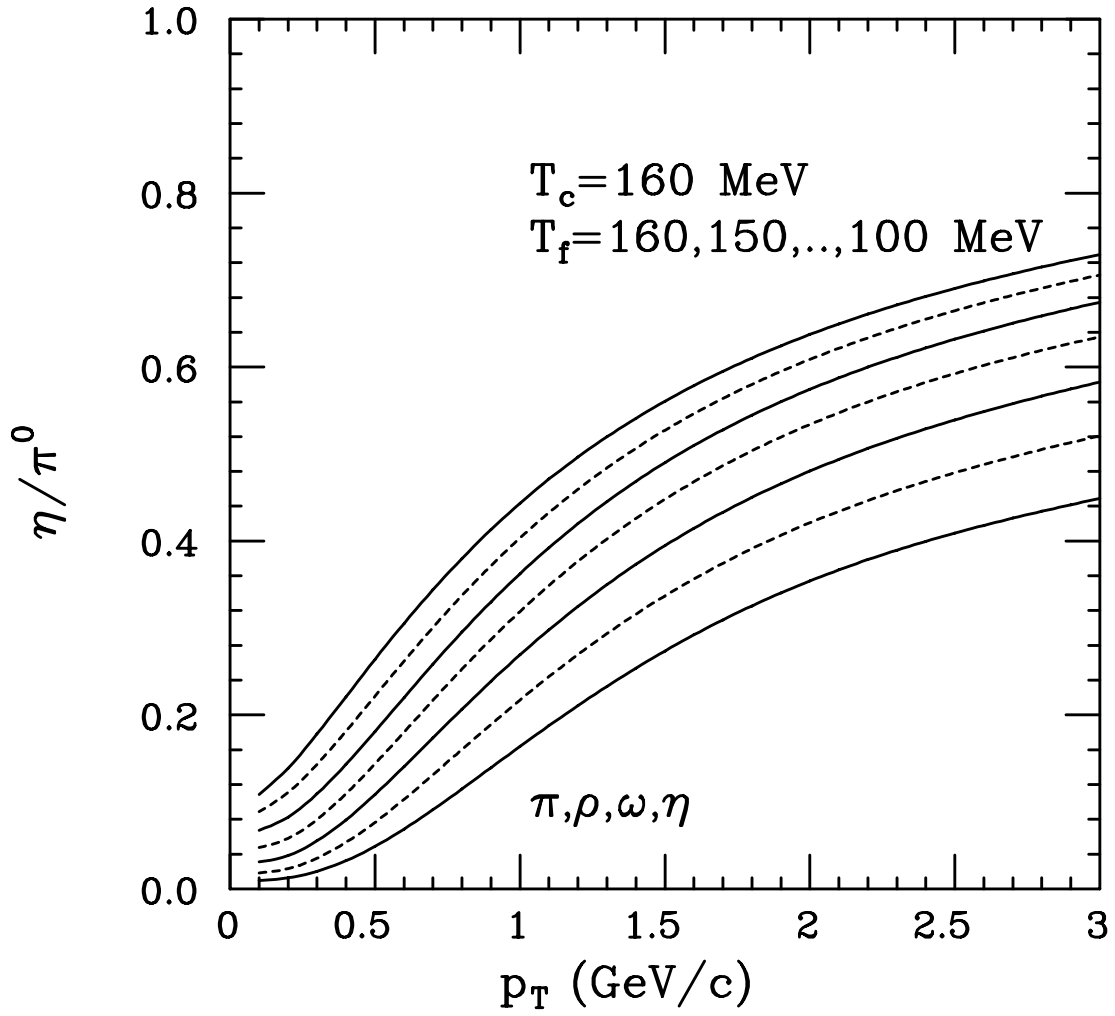
# Thermal Photons, Pb+Pb, SPS



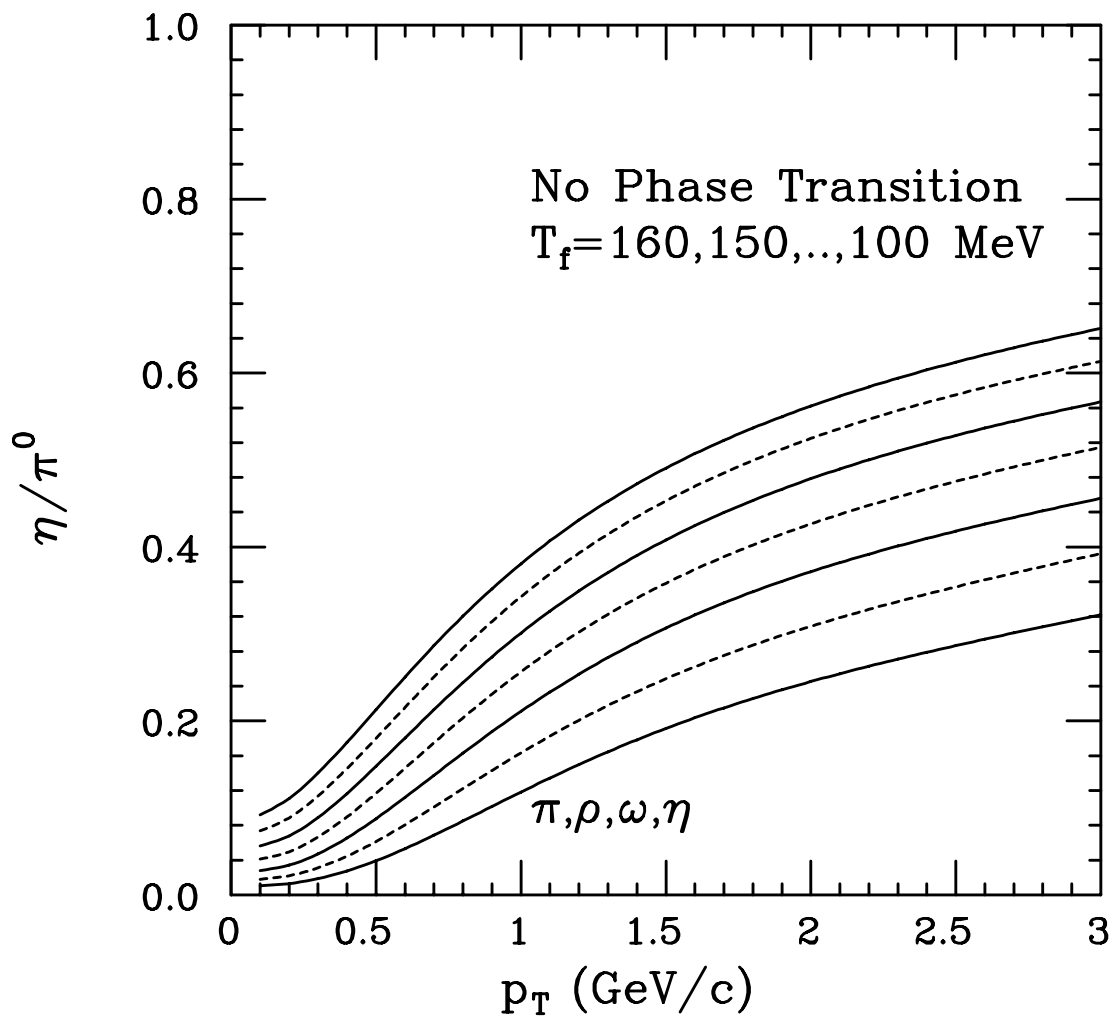
# Thermal Photons, Pb+Pb, SPS



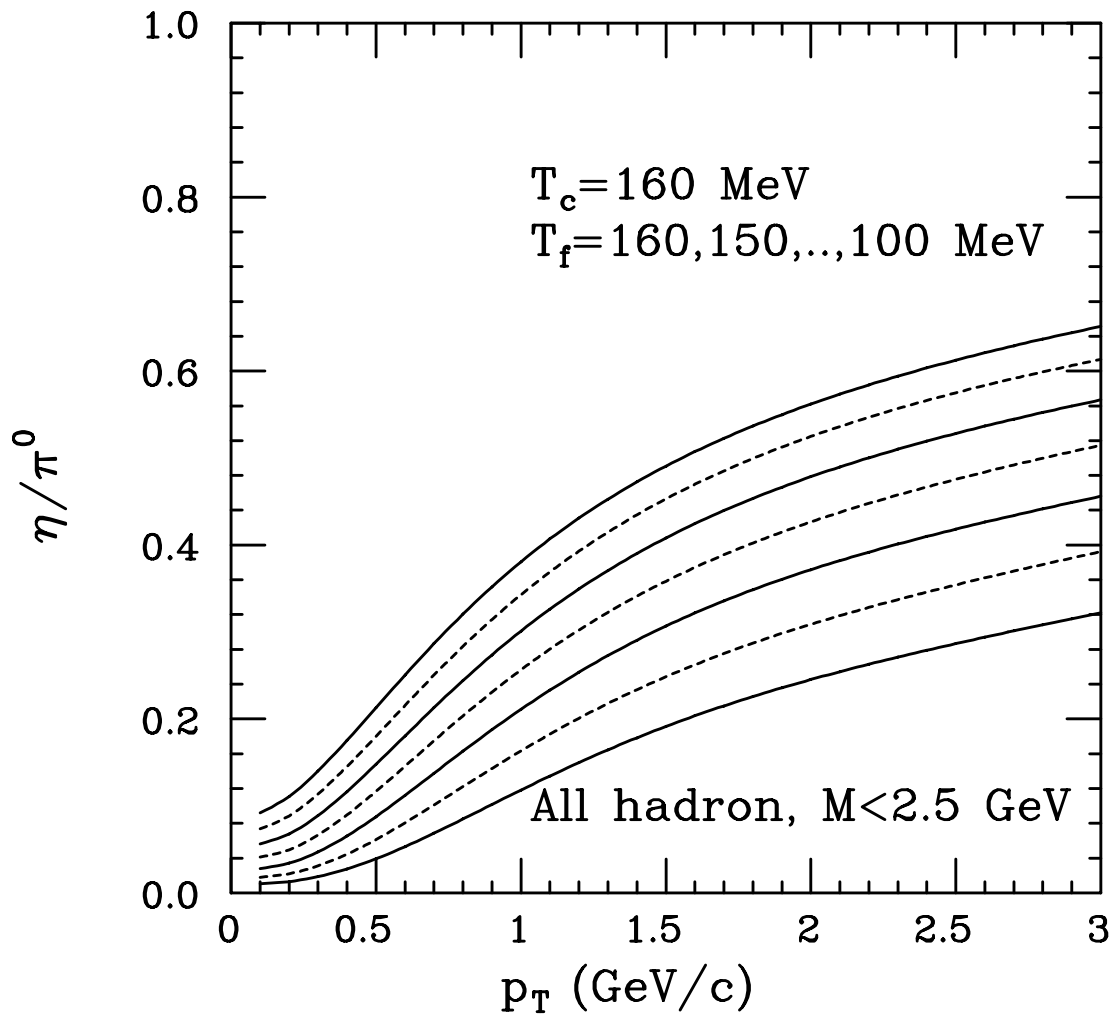
$\eta/\pi^0$  - Ratio



$\eta/\pi^0$  - Ratio



$\eta/\pi^0$  - Ratio





$\eta/\pi^0$  - Ratio

